

FAST IMEX TIME INTEGRATION OF NONLINEAR STIFF FRACTIONAL DIFFERENTIAL EQUATIONS*

YONGTAO ZHOU[†], JORGE L. SUZUKI[‡], CHENGJIAN ZHANG[§], AND MOHSEN ZAYERNOURI[¶]

Abstract. Efficient long-time integration of nonlinear fractional differential equations is significantly challenging due to the integro-differential nature of the fractional operators. In addition, the inherent non-smoothness introduced by the inverse power-law kernels deteriorates the accuracy and efficiency of many existing numerical methods. We develop two efficient first- and second-order implicit-explicit (IMEX) methods for accurate time-integration of stiff/nonlinear fractional differential equations with fractional order $\alpha \in (0, 1]$ and prove their convergence and linear stability properties. The developed methods are based on a linear multi-step fractional Adams-Moulton method (FAMM), followed by the extrapolation of the nonlinear force terms. In order to handle the singularities nearby the initial time, we employ Lubich-like corrections to the resulting fractional operators. The obtained linear stability regions of the developed IMEX methods are larger than existing IMEX methods in the literature. Furthermore, the size of the stability regions increase with the decrease of fractional order values, which is suitable for stiff problems. We also rewrite the resulting IMEX methods in the language of nonlinear Toeplitz systems, where we employ a fast inversion scheme to achieve a computational complexity of $\mathcal{O}(N \log N)$, where N denotes the number of time-steps. Our computational results demonstrate that the developed schemes can achieve global first- and second-order accuracy for highly-oscillatory stiff/nonlinear problems with singularities.

Key words. stiff/nonlinear fractional differential equations, IMEX methods, correction terms, convergence, linear stability, Toeplitz matrix

AMS subject classifications. 26A33, 34A08, 65L05, 65L12, 65L20

1. Introduction. Fractional differential equations (FDEs) have been widely applied in a variety of scientific fields, where the observed data presents the trademark of power-laws/heavy-tailed statistics across many length/time scales. Some applications include, *e.g.*, anomalous models for bio-tissues [32–34], food rheology [11, 19, 51] and earth sciences [62]. Regarding nonlinear FDEs for anomalous transport/materials, we outline fractional Navier-Stokes equations [64], fractional phase-field equations [42], complex constitutive laws applied to structural problems undergoing large deformations/strains [48] as well as nonlinear vibrations of beams [50].

Obtaining closed forms for linear FDEs can be challenging, especially for any general form of $f(t)$. In the few instances when the corresponding solution $u(t)$ is known, it is usually impractical to be numerically evaluated. Furthermore, obtaining analytical solutions becomes impossible in the presence of nonlinearities. Therefore, a series

*

Funding: This work is supported by NSFC (Grant No. 11971010), AFOSR YIP (award No. FA9550-17-1-0150), MURI/ARO (award No. W911NF-15-1-0562), ARO YIP (award No. W911NF-19-1-0444) and the NSF (award No. DMS-1923201). The work of the first author is supported by the China Scholarship Council under 201806160054.

[†]School of Mathematics and Statistics, Huazhong University of Science and Technology, Wuhan 430074, China and Department of Mechanical Engineering, Michigan State University, East Lansing, MI 48824, USA (yongtaozh@126.com).

[‡]Department of Mechanical Engineering, Michigan State University, East Lansing, MI 48824, USA (suzukijo@msu.edu, suzukijo@egr.msu.edu).

[§]School of Mathematics and Statistics, Huazhong University of Science and Technology, Wuhan 430074, China, and Hubei Key Laboratory of Engineering Modeling and Scientific Computing, Huazhong University of Science and Technology, Wuhan 430074, China (cjzhang@mail.hust.edu.cn)

[¶]Department of Mechanical Engineering and Department of Statistics and Probability, Michigan State University, East Lansing, MI 48824, USA (zayern@msu.edu, zayern@egr.msu.edu), Corresponding Author.

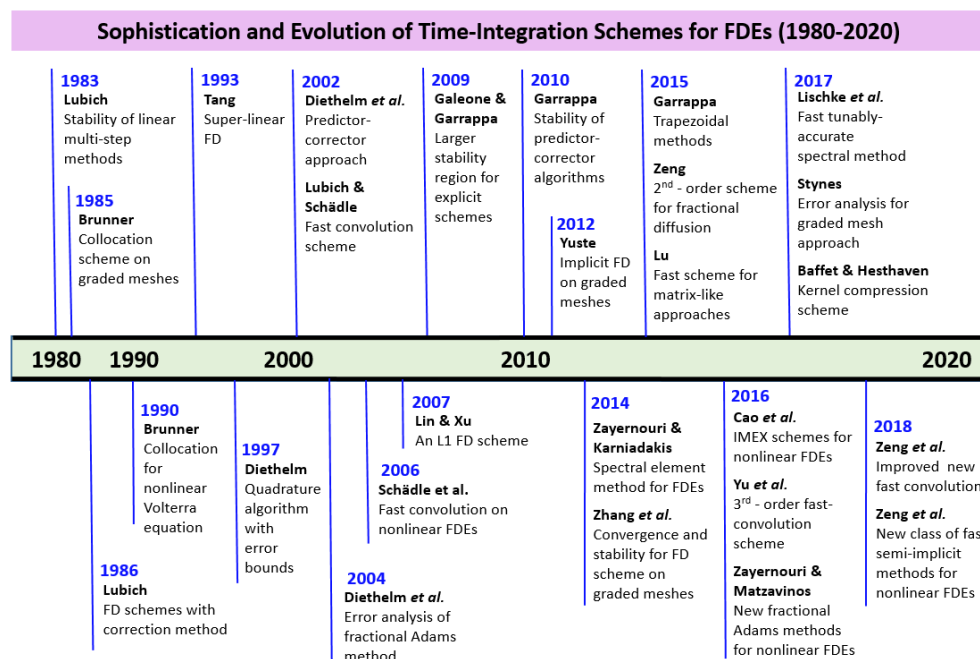


FIG. 1. Research timeline on significant and diverse numerical schemes for time-fractional differential equations.

of numerical methods for FDEs were developed since the 80's, with several significant contributions summarized in Figure 1. In such schemes it is fundamental to incorporate the history effects arising from the fractional operators. The pioneering works are attributed to Lubich [27, 28], on *discretized fractional calculus* in the sense of fractional multi-step and finite-difference (FD) schemes. Later on, Tang [49] developed a super-linear convergent FD scheme, followed by a numerical quadrature approach for fractional derivatives introduced by Diethelm [8]. In the 2000's, Diethelm developed a predictor-corrector approach in addition to a fractional Adams method [9, 10]. Later on, Lin and Xu [24] developed a FD discretization with order $2 - \alpha$, which was applied to the time-fractional diffusion equation. More recently, Garrappa [16] developed trapezoidal methods for fractional multi-step approaches and Zeng [58] developed a second-order scheme for time-fractional diffusion equations. Spectral methods were also developed in the context of FDEs/FPDEs [21, 23, 37, 39, 40, 45, 54–56, 67], and distributed-order differential equations [20, 22, 38]. In particular, Zayernouri and Karniadakis [55] developed an exponentially-accurate spectral element method for FDEs and Lischke *et al.* [25] developed a fast, *tunably-accurate* spectral method.

It is known that time-fractional operators possess power-law kernels with a singularity nearby the initial time, which produces non-smooth solutions that deteriorate the accuracy of many existing numerical schemes. In order to handle such problem, Lubich [28] introduced the *so-called* correction method, which was later applied to a series of direct/multi-step schemes for linear/nonlinear FDEs [6, 59–61], and also employed in a *self-singularity-capturing* approach by Suzuki and Zayernouri [47]. In the aforementioned works, the correct determination of singularity powers leads to

global high accuracy of the numerical schemes. The idea of *graded meshes* was also introduced with the same objectives by Brunner [4], who developed a spline collocation scheme for Volterra integro-differential equations, where the graded meshes correspond to non-uniform time-grids which are simple to incorporate in existing FD schemes. Graded meshes were later applied to nonlinear Volterra integral equations [5]. An implicit FD approach was developed in the context of graded meshes by Yuste [53]. More recently, stability issues of existing/new FD approaches were addressed by Zhang *et al.* [63] for the time-fractional diffusion equation, and also by Stynes [43] for a reaction-diffusion problem, where, in the latter, an optimal mesh grading parameter was obtained. For a comparison between the performance of Lubich's corrections and graded meshes, we refer the readers to [59].

The main computational challenge of direct FD schemes for time-integration of FDEs is the evaluation of the history term, which usually leads to a computational complexity of $\mathcal{O}(N^2)$ and memory storage of $\mathcal{O}(N)$, where N represents the total number of time-steps. To address such issues, fast schemes were developed, starting with the first-order *fast convolution method* by Lubich and Schädle [30], which reduced the computational complexity to $\mathcal{O}(N \log N)$, and memory requirements to $\mathcal{O}(\log N)$. The main idea of the scheme is to approximate the power-law kernel *via* numerical inverse Laplace transforms and split the integral operator (but not the time-grid) into exponentially increasing time steps. Later on, Schädle *et al.* [41] extended the developed fast convolution for nonlinear FDEs. A third-order extension was developed by Yu *et al.* [52] and applied to the time-integration for 3D simulation of a class of time-fractional PDEs. Zeng *et al.* [59] developed an improved version of the fast-convolution approach, which considers real-valued integration contours with the order $3 - \alpha$. Of particular interest, fast matrix-based schemes were also developed, such as the fast-inversion approach by Lu [26] and the kernel compression method by Baffet and Hesthaven [3]. The main idea of such approaches is to represent the time-stepping equation in a global linear system and exploit the resulting Toeplitz-like structure through Fast-Fourier-Transforms (FFTs).

In addition to the aforementioned challenges, dealing with stiff/nonlinear problems further deteriorates the accuracy and might pose stability issues to existing numerical schemes. Fractional linear multi-step approaches become interesting alternatives to handle such issues. Diethelm [9] developed a predictor-corrector scheme and later analyzed the error of a family of fractional Adams-Bashforth/Moulton schemes [10]. Galeone and Garrappa studied the stability of implicit and explicit fractional multi-step methods [12, 13] and proposed new explicit schemes with larger stability regions. In addition, the stability analysis of fractional predictor-corrector schemes was studied by Garrappa [15]. Also in the context fractional multi-step schemes, Zayernouri and Matzavinos [57] developed a family of fractional Adams schemes for high-order explicit/implicit treatment of nonlinear problems, where a particular time-splitting preserved the original structure of integer-order Adams schemes. Larger stability regions can be obtained through semi-implicit schemes, where for instance, Cao *et al.* [6] developed two IMEX schemes for nonlinear FDEs, utilizing two distinct force extrapolation formulas and also analyzed the stability of the developed schemes. Recently, Zeng *et al.* [60] developed a new class of fast, second-order semi-implicit methods for nonlinear FDEs through new fast convolutions. Zhou and Zhang also developed and analyzed the convergence and stability of one-leg approaches [66] and a class of boundary value methods and their block version [65, 68] for stiff/nonlinear FDEs.

Although a significant amount of relevant works was developed, they usually ad-

dress the aforementioned singularity/performance/stability issues for stiff/nonlinear problems separately. In this regard, there is still a need for numerical schemes in the context of stiff/nonlinear FDEs that **I**) efficiently handle the numerical solution with low-regularity for both the solution $u(t)$ and nonlinear term $f(t, u(t))$; **II**) present linear complexity with respect to the number of time-steps N ; **III**) have larger stability regions compared to the existing numerical schemes; **IV**) mimic and generalize the structure of existing integer-order IMEX schemes, widely employed by the scientists and engineers to its fractional-order counterparts. The main contribution of the present work is to develop a class of IMEX methods for accurate time-integration of stiff/nonlinear FDEs. Specifically:

- We start with the linear multi-step FAMMs developed by Zayernouri and Matzavinos [57] in the sense of linear/nonlinear fractional Cauchy equations. For the linear problem, two sets of Lubich-like correction terms [28] are employed.
- We develop a class of new first- and second-order IMEX methods with the combination of Zayernouri and Matzavinos [57] FAMMs with two extrapolation methods for the nonlinear term. The obtained methods are denoted by IMEX(p), which is first-order accurate when $p = 0$, and second-order accurate when $p = 1$.
- The convergence and linear stability of the developed IMEX methods are proved and the corresponding regions of stability are shown to be larger for smaller values of the fractional order α .
- The convolution nature of the fractional operators allows us to represent the corresponding IMEX methods in the language of global-in-time Toeplitz-like nonlinear systems, and employ the fast approximate inversion approach by Lu *et al.* [26]. Since the Toeplitz system is nonlinear, we utilize a Picard iteration scheme which takes N^p iterations until convergence with respect to a specified tolerance ϵ^p . Under suitable conditions, N^p does not significantly increase with N .
- The corresponding *history load* for the developed IMEX schemes is given by hypergeometric functions, which are efficiently evaluated through a Gauss-Jacobi quadrature with a fixed number of Q integration points.
- The asymptotic computational complexity of the scheme is $\mathcal{O}(N \log N)$, with memory storage of order $\mathcal{O}(N)$.

This paper is organized as follows: Section 2 follows a step-by-step procedure, starting with linear multi-step FAMMs for linear FDEs, up to nonlinear FDEs, when the developed IMEX methods will be introduced. In Section 3 we demonstrate the linear stability of the developed IMEX methods. In Section 4 we put the corresponding IMEX methods in the language of a global nonlinear system of equations and employ a fast solver. The numerical results for linear/nonlinear/stiff FDEs with discussions are shown in Section 5, followed by the Conclusions in Section 6.

2. Implicit-Explicit Time-Integration Methods. We develop two IMEX methods for efficient time-integration of nonlinear FDEs. In a step-by-step fashion, we start with the numerical solution of a fractional linear Cauchy problem, following the idea of FAMMs proposed by Zayernouri and Matzavinos in [57]. To capture the singularity of the solution $u(t)$ of the considered problem, we then develop two sets of appropriate correction terms by using Lubich's approach [28] for the resulting fractional operators. As a next step, we introduce a nonlinear forcing term $f(t, u(t))$ and develop two IMEX methods for the solution of the resulting nonlinear Cauchy prob-

lem, which also introduces two additional sets of correction weights due to $f(t, u(t))$.

2.1. Definitions. We start with some preliminary definitions for fractional calculus (see e.g. [36]). The left-sided Caputo fractional derivative of order α ($0 < \alpha < 1$) is defined by

$$(1) \quad {}^C D_t^\alpha u(t) = {}_{t_L} I_t^{1-\alpha} u'(t) = \frac{1}{\Gamma(1-\alpha)} \int_{t_L}^t \frac{u'(v)}{(t-v)^\alpha} dv, \quad t > t_L,$$

where $\Gamma(\cdot)$ denotes the usual gamma function. The operator ${}_{t_L} I_t^\alpha$ represents the α -th order ($0 < \alpha < 1$) left-sided fractional Riemann-Liouville (RL) integral operator, defined as

$$(2) \quad {}_{t_L} I_t^\alpha u(t) = \frac{1}{\Gamma(\alpha)} \int_{t_L}^t \frac{u(v)}{(t-v)^{1-\alpha}} dv, \quad t > t_L.$$

The corresponding inverse operator of (2), *i.e.*, the left-sided Riemann-Liouville fractional derivative of order α is denoted by

$$(3) \quad {}^{RL} D_t^\alpha u(t) = \frac{d}{dt} [{}_{t_L} I_t^\alpha u(t)] = \frac{1}{\Gamma(1-\alpha)} \frac{d}{dt} \int_{t_L}^t \frac{u(v)}{(t-v)^\alpha} dv, \quad t > t_L.$$

Moreover, the left-sided Caputo fractional derivative and the left-sided Riemann-Liouville fractional derivative are linked by the following relationship:

$$(4) \quad {}^{RL} D_t^\alpha u(t) = \frac{u(t_L)}{\Gamma(1-\alpha)(t-t_L)^\alpha} + {}^C D_t^\alpha u(t).$$

2.2. Linear FDEs. Consider the numerical solutions of the following linear FDE:

$$(5) \quad {}^C D_t^\alpha u(t) = \lambda u(t), \quad \alpha \in (0, 1], \quad t \in (0, T]; \quad u(0) = u_0,$$

where $\lambda \in \mathbb{C}$, $u_0 \in \mathbb{R}^d$. Now, we adopt the FAMMs developed in [57] to solve (5). Let $h > 0$ be the time-step size with $h = T/N$ ($N \in \mathbb{N}$) and $t_k = kh$ ($0 \leq k \leq N$). By the definition of the Caputo fractional derivative (1), we can split the fractional operator in history and local parts:

$$(6) \quad \begin{aligned} {}^C D_t^\alpha u(t) &= \frac{1}{\Gamma(1-\alpha)} \int_0^{t_k} \frac{u'(v)}{(t-v)^\alpha} dv + \frac{1}{\Gamma(1-\alpha)} \int_{t_k}^t \frac{u'(v)}{(t-v)^\alpha} dv \\ &:= H^k(t) + {}^C D_{t_k}^\alpha u(t). \end{aligned}$$

Moreover, from (4), we have

$$(7) \quad {}^C D_{t_k}^\alpha u(t) = {}^C D_{t_k}^\alpha [u(t) - u(t_k) + u(t_k)] = {}^C D_{t_k}^\alpha [u(t) - u(t_k)] = {}^{RL} D_{t_k}^\alpha [u(t) - u(t_k)].$$

Then, by substituting (6) and (7) into (5), it holds that

$$(8) \quad {}^{RL} D_{t_k}^\alpha [u(t) - u(t_k)] = \lambda u(t) - H^k(t), \quad \alpha \in (0, 1], \quad t \in (0, T].$$

Applying the inverse operator ${}_{t_k} I_t^\alpha$ on the both sides of (8) and evaluating at $t = t_{k+1}$, we obtain

$$(9) \quad u(t_{k+1}) - u(t_k) = [\lambda {}_{t_k} I_t^\alpha u(t) - \mathcal{H}^k(t)] \Big|_{t=t_{k+1}},$$

where $\mathcal{H}^k(t)$ denotes the *history load term*, which is given by:

$$(10) \quad \mathcal{H}^k(t) = {}_{t_k}I_t^\alpha(H^k(t)) = \frac{1}{\Gamma(\alpha)\Gamma(1-\alpha)} \int_{t_k}^t \frac{1}{(t_{k+1}-v)^{1-\alpha}} \int_0^{t_k} \frac{u'(s)}{(v-s)^\alpha} ds dv.$$

We follow the FAMMs from [57] and interpolate $u(t)$ from ${}_{t_k}I_t^\alpha u(t)\Big|_{t=t_{k+1}}$ in an implicit fashion:

$$(11) \quad {}_{t_k}I_t^\alpha u(t)\Big|_{t=t_{k+1}} \approx h^\alpha \sum_{j=0}^p \beta_j^{(p)} u(t_{k+1-j}), \quad p = 0, 1,$$

with the following fractional Adams-Moulton coefficients, respectively, for $p = 0$ and $p = 1$,

$$\beta_0^{(0)} = \frac{1}{\Gamma(\alpha+1)}; \quad \beta_0^{(1)} = \frac{1}{\Gamma(\alpha+2)}, \quad \beta_1^{(1)} = \frac{\alpha}{\Gamma(\alpha+2)}.$$

Moreover, these coefficients recover the standard Adams-Moulton method's coefficients in the limit case when $\alpha = 1$. To compute the history load term $\mathcal{H}^k(t_{k+1})$, on each small interval $[t_j, t_{j+1}]$ ($0 \leq j \leq k-1$), we linearly interpolate $u(t)$ when $p = 0$, as follows:

$$\Pi_{1,j}u(t) = \frac{t-t_{j+1}}{t_j-t_{j+1}}u(t_j) + \frac{t-t_j}{t_{j+1}-t_j}u(t_{j+1}),$$

therefore, we obtain the following form for the history load:

$$(12) \quad \mathcal{H}^k(t_{k+1}) \approx \mathcal{H}_0^k(t_{k+1}) = \frac{1}{\Gamma(\alpha)\Gamma(2-\alpha)} \sum_{j=0}^{k-1} \frac{u(t_{j+1})-u(t_j)}{h} (\mathcal{A}_{k,j} - \mathcal{A}_{k,j+1}),$$

where

$$(13) \quad \begin{aligned} \mathcal{A}_{k,j} &= \int_{t_k}^{t_{k+1}} (t_{k+1}-v)^{\alpha-1} (v-t_j)^{1-\alpha} dv = h \int_0^1 (1-\theta)^{\alpha-1} (k-j+\theta)^{1-\alpha} d\theta \\ &= h \begin{cases} \frac{(k-j)^{1-\alpha}}{\alpha} {}_2F_1\left(\alpha-1, 1; \alpha+1; \frac{1}{j-k}\right), & 0 \leq j < k, \\ \Gamma(\alpha)\Gamma(2-\alpha), & j = k, \end{cases} \end{aligned}$$

in which ${}_2F_1(a, b; c; z)$ denotes the hypergeometric function. Also, when $p = 1$, we utilize quadratic interpolation function $\Pi_{2,j}u(t)$ to approximate $u(t)$ on the interval $[t_j, t_{j+1}]$ ($0 \leq j \leq k-1$) as follows:

$$\begin{aligned} \Pi_{2,j}u(t) &= \frac{(t-t_j)(t-t_{j+1})}{(t_{j-1}-t_j)(t_{j-1}-t_{j+1})}u(t_{j-1}) + \frac{(t-t_{j-1})(t-t_{j+1})}{(t_j-t_{j-1})(t_j-t_{j+1})}u(t_j) \\ &\quad + \frac{(t-t_{j-1})(t-t_j)}{(t_{j+1}-t_{j-1})(t_{j+1}-t_j)}u(t_{j+1}), \end{aligned}$$

and therefore, the history load for the choice of $p = 1$ is given by

$$(14) \quad \begin{aligned} \mathcal{H}^k(t_{k+1}) &\approx \mathcal{H}_1^k(t_{k+1}) = \mathcal{H}_0^k(t_{k+1}) \\ &+ \frac{1}{\Gamma(\alpha)\Gamma(2-\alpha)} \sum_{j=1}^{k-1} \frac{u(t_{j+1})-2u(t_j)+u(t_{j-1}))}{h^2} \left[-\frac{h(\mathcal{A}_{k,j}+\mathcal{A}_{k,j+1})}{2} + \frac{\mathcal{B}_{k,j}-\mathcal{B}_{k,j+1}}{2-\alpha} \right], \end{aligned}$$

where

$$(15) \quad \begin{aligned} \mathcal{B}_{k,j} &= \int_{t_k}^{t_{k+1}} (t_{k+1} - v)^{\alpha-1} (v - t_j)^{2-\alpha} dv = h^2 \int_0^1 (1-\theta)^{\alpha-1} (k-j+\theta)^{2-\alpha} d\theta \\ &= h^2 \begin{cases} \frac{(k-j)^{2-\alpha}}{\alpha} {}_2F_1\left(\alpha-2, 1; \alpha+1; \frac{1}{j-k}\right), & 0 \leq j < k, \\ \frac{\Gamma(\alpha)\Gamma(3-\alpha)}{2}, & j = k. \end{cases} \end{aligned}$$

Let u_k be the approximate solution of $u(t_k)$ ($0 \leq k \leq N$), and denote

$$(16) \quad \mathcal{H}_p^k = \frac{1}{\Gamma(\alpha)\Gamma(2-\alpha)} \sum_{j=0}^k \gamma_{k,j}^{(p)} u_j, \quad p = 0, 1,$$

where the coefficients $\gamma_{k,j}^{(p)}$ are presented in Appendix A. Then, we get the FAMMs for (9) have the following discrete form:

$$(17) \quad \frac{u_{k+1} - u_k}{h^\alpha} = \lambda \sum_{j=0}^p \beta_j^{(p)} u_{k+1-j} - \frac{1}{h^\alpha} \mathcal{H}_p^k, \quad p = 0, 1.$$

In order to lay the analytical basis for the convergence and linear stability analysis of the methods, we introduce several preparatory results through a series of lemmas, with their corresponding proofs given in Appendix B.

LEMMA 1. *The coefficients $\{\gamma_{k,j}^{(p)}\}$ in (16) have the following properties for $0 \leq j \leq k$, $0 \leq k \leq N$ and $p = 0, 1$:*

- $\gamma_{k,j}^{(0)} < 0$ ($0 \leq j \leq k-1$), $0 < \gamma_{k,k}^{(0)} \leq C_1$;
- $\gamma_{k,j}^{(1)} < 0$ ($0 \leq j \leq k-3$), $|\gamma_{k,j}^{(1)}| \leq C_1$ ($j = k-2, k-1$ or k);
- $\sum_{j=0}^k \gamma_{k,j}^{(0)} = 0$, $\sum_{j=0}^k \gamma_{k,j}^{(1)} = 0$,

where $C_1 > 0$ is a constant.

LEMMA 2. *Let $u(t) = t^\sigma$ ($\sigma \geq 0$). Then there exists a constant $C_2 > 0$ independent of h such that*

$$\left| {}_{t_k} I_t^\alpha u(t) \Big|_{t=t_{k+1}} - h^\alpha \sum_{j=0}^p \beta_j^{(p)} u(t_{k+1-j}) \right| \leq C_2 h^{\alpha+p+1} t_{k+1}^{\sigma-p-1}.$$

LEMMA 3. *Let $u(t) = t^\sigma$ ($\sigma \geq 0$). Then there exists a constant $C_3 > 0$ independent of h such that*

$$\left| \mathcal{H}^k(t_{k+1}) - \mathcal{H}_p^k(t_{k+1}) \right| \leq C_3 \left(h^{\sigma+\alpha+1} t_{k+1}^{-\alpha-1} + h^{\alpha+p+1} t_{k+1}^{\sigma-\alpha-p-1} + h^{p+1} \right).$$

2.3. Correction Terms. It is well-known that the solutions of (5) usually exhibit weak singularity at the initial time. Hence, the optimal convergence rates of the above discussed numerical methods cannot be achieved (see Lemma 2 and 3). To improve the accuracy near the initial time, we follow Lubich's idea (cf. [28]) by adding correction terms to the resulting fractional operators of (9). The correction

scheme assumes that the solution $u(t)$ of (5) has the form (see e.g. [6, 10, 61] for more discussions on the regularity of FDEs):

$$(18) \quad u(t) - u(0) = \sum_{r=1}^{m+1} d_r t^{\sigma_r} + \zeta(t) t^{\sigma_{m+2}}, \quad 0 < \sigma_r < \sigma_{r+1},$$

where $d_r \in \mathbb{R}$ are some constants, m is a positive integer and $\zeta(t)$ is a uniformly continuous function for $t \in [0, T]$. The term $\{\sigma_r\}$ represents positive correction powers. We will now introduce the correction approach for each term of the right-hand-side of (9).

I) We start with the term ${}_t I_t^\alpha u(t) \Big|_{t=t_{k+1}}$. It follows from Lemma 2 that

$$(19) \quad \begin{aligned} {}_t I_t^\alpha u(t) \Big|_{t=t_{k+1}} &= {}_{t_k} I_t^\alpha (u(t) - u(0)) \Big|_{t=t_{k+1}} + {}_t I_t^\alpha u(0) \Big|_{t=t_{k+1}} \\ &= h^\alpha \sum_{j=0}^p \beta_j^{(p)} (u(t_{k+1-j}) - u_0) + h^\alpha \sum_{j=1}^{m_u} W_{k,j}^{(\alpha, \sigma, p)} (u(t_j) - u_0) \\ &\quad + \frac{h^\alpha}{\Gamma(\alpha + 1)} u_0 + R_{k+1}^u \\ &= h^\alpha \sum_{j=0}^p \beta_j^{(p)} u(t_{k+1-j}) + h^\alpha \sum_{j=1}^{m_u} W_{k,j}^{(\alpha, \sigma, p)} (u(t_j) - u_0) + R_{k+1}^u \\ &:= h^\alpha I_{h, m_u}^{\alpha, \sigma, p} u(t_{k+1}) + R_{k+1}^u, \end{aligned}$$

with $R_{k+1}^u = \mathcal{O}(h^{\alpha+p+1} t_{k+1}^{\sigma_{m_u+1}-p-1})$. The correction weights $\{W_{k,j}^{(\alpha, \sigma, p)}\}$ are chosen such that (19) is exact for $u(t) = t^{\sigma_r}$ ($1 \leq r \leq m_u$), and therefore are obtained through the following linear system of order $m_u \times m_u$ to be solved for $k = 0, 1, \dots, N-1$ time steps:

$$(20) \quad \sum_{j=1}^{m_u} W_{0,j}^{(\alpha, \sigma, p)} j^{\sigma_r} = \frac{\Gamma(\sigma_r + 1)}{\Gamma(\sigma_r + \alpha + 1)} - \sum_{j=0}^p \beta_j^{(p)} (1-j)^{\sigma_r}, \quad 1 \leq r \leq m_u,$$

$$(21) \quad \begin{aligned} \sum_{j=1}^{m_u} W_{k,j}^{(\alpha, \sigma, p)} j^{\sigma_r} &= \frac{k^{\sigma_r}}{\Gamma(\alpha + 1)} {}_2F_1 \left(-\sigma_r, 1; \alpha + 1; -\frac{1}{k} \right) - \sum_{j=0}^p \beta_j^{(p)} (k+1-j)^{\sigma_r}, \\ &1 \leq k \leq N-1, \quad 1 \leq r \leq m_u. \end{aligned}$$

II) For the history load $\mathcal{H}^k(t_{k+1})$, we introduce the correction terms as follows. Substituting (18) into (10) and using Lemma 3 yield

$$\begin{aligned} \mathcal{H}^k(t_{k+1}) &= \frac{1}{\Gamma(\alpha)\Gamma(1-\alpha)} \int_{t_k}^{t_{k+1}} \frac{1}{(t_{k+1}-v)^{1-\alpha}} \int_0^{t_k} \frac{[u(s) - u(0)]'}{(v-s)^\alpha} ds dv \\ &\quad + \frac{1}{\Gamma(\alpha)\Gamma(1-\alpha)} \int_{t_k}^{t_{k+1}} \frac{1}{(t_{k+1}-v)^{1-\alpha}} \int_0^{t_k} \frac{u'(0)}{(v-s)^\alpha} ds dv \\ &= \frac{1}{\Gamma(\alpha)\Gamma(2-\alpha)} \sum_{j=0}^k \gamma_{k,j}^{(p)} u(t_j) + \sum_{j=1}^{\tilde{m}_u} \tilde{W}_{k,j}^{(\alpha, \sigma, p)} (u(t_j) - u_0) + \tilde{R}_{k+1}^u \end{aligned}$$

$$(22) \quad := \mathcal{H}_{\tilde{m}_u}^{\alpha, \sigma, p} u(t_{k+1}) + \tilde{R}_{k+1}^u,$$

with $\tilde{R}_{k+1}^u = \mathcal{O}(h^{\sigma \tilde{m}_u + 1 + \alpha + 1} t_{k+1}^{-\alpha - 1}) + \mathcal{O}(h^{\alpha + p + 1} t_{k+1}^{\sigma \tilde{m}_u + 1 - \alpha - p - 1}) + \mathcal{O}(h^{p+1})$. The history load correction weights $\{\tilde{W}_{k,j}^{(\alpha, \sigma, p)}\}$ are chosen such that (22) is exact for $u(t) = t^{\sigma r}$ ($1 \leq r \leq \tilde{m}_u$). However, we remark that it is very difficult to obtain the analytical solution of $\mathcal{H}^k(t_{k+1})$, given $u(t) = t^{\sigma r}$. Fortunately, we know from [7] that (9) is also equivalent to

$$(23) \quad \begin{aligned} u(t_{k+1}) = & u(t_k) + \frac{\lambda}{\Gamma(\alpha)} \int_{t_k}^{t_{k+1}} (t_{k+1} - v)^{\alpha-1} u(v) dv \\ & + \frac{\lambda}{\Gamma(\alpha)} \int_0^{t_k} [(t_{k+1} - v)^{\alpha-1} - (t_k - v)^{\alpha-1}] u(v) dv. \end{aligned}$$

Comparing (9) with (23) and using (5), we can obtain

$$(24) \quad \begin{aligned} \mathcal{H}^k(t_{k+1}) = & - \frac{\lambda}{\Gamma(\alpha)} \int_0^{t_k} [(t_{k+1} - v)^{\alpha-1} - (t_k - v)^{\alpha-1}] u(v) dv \\ = & - \frac{1}{\Gamma(\alpha)} \int_0^{t_k} [(t_{k+1} - v)^{\alpha-1} - (t_k - v)^{\alpha-1}] {}_0^C D_t^\alpha u(v) dv. \end{aligned}$$

Therefore, we have the following linear system of size $\tilde{m}_u \times \tilde{m}_u$ to be solved for $k = 1, 2, \dots, N-1$ time steps:

$$(25) \quad \begin{aligned} \sum_{j=1}^{\tilde{m}_u} \tilde{W}_{k,j}^{(\alpha, \sigma, p)} j^{\sigma r} = & k^{\sigma r} - \frac{\Gamma(\sigma_r + 1)}{\Gamma(\alpha) \Gamma(\sigma_r - \alpha + 1)} (k+1)^{\sigma_r} B\left(\frac{k}{k+1}; \sigma_r - \alpha + 1, \alpha\right) \\ & - \frac{1}{\Gamma(\alpha) \Gamma(2 - \alpha)} \sum_{j=0}^k \gamma_{k,j}^{(p)} j^{\sigma r}, \quad 1 \leq k \leq N-1, \quad 1 \leq r \leq \tilde{m}_u, \end{aligned}$$

where $B(z; a, b)$ denotes the incomplete beta function, which is defined by

$$B(z; a, b) = \int_0^z v^{a-1} (1-v)^{b-1} dv.$$

Substituting (19) and (22) into (9) yields

$$(26) \quad u(t_{k+1}) = u(t_k) + \lambda h^\alpha I_{h, m_u}^{\alpha, \sigma, p} u(t_{k+1}) - \mathcal{H}_{\tilde{m}_u}^{\alpha, \sigma, p} u(t_{k+1}) + R_{k+1}^u + \tilde{R}_{k+1}^u, \quad p = 0, 1.$$

Dropping the truncation errors R_{k+1}^u and \tilde{R}_{k+1}^u in (26) and replacing $u(t_k)$ with approximate solution u_k , we obtain the following FAMMs with correction terms for solving (5):

$$(27) \quad \frac{u_{k+1} - u_k}{h^\alpha} = \lambda I_{h, m_u}^{\alpha, \sigma, p} u_{k+1} - \frac{1}{h^\alpha} \mathcal{H}_{\tilde{m}_u}^{\alpha, \sigma, p} u_{k+1}, \quad p = 0, 1,$$

with $I_{h, m_u}^{\alpha, \sigma, p} u_{k+1}$ and $\mathcal{H}_{\tilde{m}_u}^{\alpha, \sigma, p} u_{k+1}$ given, respectively, by:

$$(28) \quad I_{h, m_u}^{\alpha, \sigma, p} u_{k+1} = \sum_{j=0}^p \beta_j^{(p)} u_{k+1-j} + \sum_{j=1}^{m_u} W_{k,j}^{(\alpha, \sigma, p)} (u_j - u_0),$$

and

$$(29) \quad \mathcal{H}_{\tilde{m}_u}^{\alpha, \sigma, p} u_{k+1} = \frac{1}{\Gamma(\alpha) \Gamma(2 - \alpha)} \sum_{j=0}^k \gamma_{k,j}^{(p)} u_j + \sum_{j=1}^{\tilde{m}_u} \tilde{W}_{k,j}^{(\alpha, \sigma, p)} (u_j - u_0).$$

2.4. Nonlinear FDEs. Having defined the discretization and corrections for the linear case, we now consider the numerical solutions of the following nonlinear FDE:

$$(30) \quad {}_0^C D_t^\alpha u(t) = \lambda u(t) + f(t, u), \quad \alpha \in (0, 1], \quad t \in (0, T]; \quad u(0) = u_0,$$

where the nonlinear function $f : (0, T] \times \mathbb{R}^d \rightarrow \mathbb{R}^d$ satisfies the Lipschitz condition with constant $L > 0$:

$$(31) \quad \|f(t, u) - f(t, \hat{u})\|_\infty \leq L \|u - \hat{u}\|_\infty, \quad t \in (0, T], \quad u, \hat{u} \in \mathbb{R}^d,$$

where $\|\cdot\|_\infty$ denotes the usual maximum norm on \mathbb{R}^d . Under these assumptions, it has been proved by Diethelm and Ford [9, Theorem 2.1 and 2.2] that problem (30) has a unique solution on the interval $(0, T]$.

By the same token, we adopt the FAMMs developed in [57] to solve (30), and in a similar fashion as Section 2.2, but with the addition of the nonlinear term $f(t, u)$, we have:

$$(32) \quad u(t_{k+1}) - u(t_k) = \left[\lambda {}_{t_k} I_t^\alpha u(t) + {}_{t_k} I_t^\alpha f(t, u) - \mathcal{H}^k(t) \right] \Big|_{t=t_{k+1}}.$$

Therefore, the FAMMs for (32) is given by:

$$(33) \quad \frac{u_{k+1} - u_k}{h^\alpha} = \sum_{j=0}^p \beta_j^{(p)} (\lambda u_{k+1-j} + f_{k+1-j}) - \frac{1}{h^\alpha} \mathcal{H}_p^k, \quad p = 0, 1,$$

where $f_{k+1-j} = f(t_{k+1-j}, u_{k+1-j})$.

2.4.1. Corrections Terms for $f(t, u)$. The regularity of $f(t, u)$ is related to the regularity of $u(t)$. If $u(t)$ satisfies (18), we know from (30) that

$$(34) \quad \begin{aligned} f(t, u) - f(0, u(0)) &= -\lambda \sum_{r=1}^{m+1} d_r t^{\sigma_r} + \sum_{r=1}^{m+1} d_r \frac{\Gamma(\sigma_r + 1)}{\Gamma(\sigma_r - \alpha + 1)} t^{\sigma_r - \alpha} + \dots \\ &:= \sum_{r=1}^{l+1} h_r t^{\delta_r} + \hat{\zeta}(t) t^{\delta_{l+2}}, \quad \delta_r < \delta_{r+1}, \end{aligned}$$

where $\hat{\zeta}(t)$ is a uniformly continuous function for $t \in [0, T]$ and $\delta_r \in \{\sigma_l\} \cup \{\sigma_l - \alpha\}$. Similar to (19) and by using Lemma 2, we have

$$(35) \quad \begin{aligned} {}_{t_k} I_t^\alpha f(t, u) \Big|_{t=t_{k+1}} &= h^\alpha \sum_{j=0}^p \beta_j^{(p)} f(t_{k+1-j}, u(t_{k+1-j})) \\ &\quad + h^\alpha \sum_{j=1}^{m_f} W_{k,j}^{(\alpha, \delta, p)} (f(t_j, u(t_j)) - f(0, u_0)) + R_{k+1}^f \\ &:= h^\alpha I_{h, m_f}^{\alpha, \delta, p} f(t_{k+1}, u(t_{k+1})) + R_{k+1}^f, \end{aligned}$$

where $R_{k+1}^f = \mathcal{O}(h^{\alpha+p+1} t_{k+1}^{\delta_{m_f+1} - p - 1})$, and $\{W_{k,j}^{(\alpha, \delta, p)}\}$ with $k = 0, 1, \dots, N-1$ and $j = 1, 2, \dots, m_f$ are given by:

$$(36) \quad \sum_{j=1}^{m_f} W_{0,j}^{(\alpha, \delta, p)} j^{\delta_r} = \frac{\Gamma(\delta_r + 1)}{\Gamma(\delta_r + \alpha + 1)} - \sum_{j=0}^p \beta_j^{(p)} (1-j)^{\delta_r}, \quad 1 \leq r \leq m_f,$$

$$(37) \quad \sum_{j=1}^{m_f} W_{k,j}^{(\alpha,\delta,p)} j^{\delta_r} = \frac{k^{\delta_r}}{\Gamma(\alpha+1)} {}_2F_1\left(-\delta_r, 1; \alpha+1; -\frac{1}{k}\right) - \sum_{j=0}^p \beta_j^{(p)} (k+1-j)^{\delta_r},$$

$$1 \leq k \leq N-1, \quad 1 \leq r \leq m_f.$$

Inserting (19), (22) and (35) into (32) yields

$$(38) \quad \begin{aligned} u(t_{k+1}) = & u(t_k) + \lambda h^\alpha I_{h,m_u}^{\alpha,\sigma,p} u(t_{k+1}) + h^\alpha I_{h,m_f}^{\alpha,\delta,p} f(t_{k+1}, u(t_{k+1})) \\ & - \mathcal{H}_{\tilde{m}_u}^{\alpha,\sigma,p} u(t_{k+1}) + R_{k+1}^u + R_{k+1}^f + \tilde{R}_{k+1}^u, \quad p = 0, 1. \end{aligned}$$

Therefore, we obtain the following FAMMs with correction terms for solving (30):

$$(39) \quad \frac{u_{k+1} - u_k}{h^\alpha} = \lambda I_{h,m_u}^{\alpha,\sigma,p} u_{k+1} + I_{h,m_f}^{\alpha,\delta,p} f_{k+1} - \frac{1}{h^\alpha} \mathcal{H}_{\tilde{m}_u}^{\alpha,\sigma,p} u_{k+1}, \quad p = 0, 1,$$

with $I_{h,m_u}^{\alpha,\sigma,p} u_{k+1}$, $\mathcal{H}_{\tilde{m}_u}^{\alpha,\sigma,p} u_{k+1}$ and $I_{h,m_f}^{\alpha,\delta,p} f_{k+1}$ given, respectively, by (28), (29) and

$$(40) \quad I_{h,m_f}^{\alpha,\delta,p} f_{k+1} = \sum_{j=0}^p \beta_j^{(p)} f_{k+1-j} + \sum_{j=1}^{m_f} W_{k,j}^{(\alpha,\delta,p)} (f_j - f_0).$$

In order to obtain the IMEX methods, we follow the idea from Cao et al. [6], and employ an extrapolation to linearize the nonlinear force term $f(t_{k+1}, u(t_{k+1}))$ in (38), which is given by:

$$(41) \quad f(t_{k+1}, u(t_{k+1})) = E_k^p f(t_k, u(t_k)) + \sum_{j=1}^{\tilde{m}_f} W_{k,j}^{(\delta,p)} (f(t_j, u(t_j)) - f(0, u_0)) + \tilde{R}_{k+1}^f,$$

where

$$(42) \quad E_k^p f(t_k, u(t_k)) = \begin{cases} f(t_k, u(t_k)), & p = 0, \\ 2f(t_k, u(t_k)) - f(t_{k-1}, u(t_{k-1})), & p = 1, \end{cases}$$

and $\tilde{R}_k^f = \mathcal{O}(h^{p+1} t_{k+1}^{\delta_{\tilde{m}_f+1}-p-1})$. In addition, the $\tilde{m}_f \times \tilde{m}_f$ linear system for correction weights is given by:

$$(43) \quad \sum_{j=1}^{\tilde{m}_f} W_{k,j}^{(\delta,0)} j^{\delta_r} = (k+1)^{\delta_r} - k^{\delta_r}, \quad 1 \leq r \leq \tilde{m}_f,$$

$$(44) \quad \sum_{j=1}^{\tilde{m}_f} W_{k,j}^{(\delta,1)} j^{\delta_r} = (k+1)^{\delta_r} - 2k^{\delta_r} + (k-1)^{\delta_r}, \quad 1 \leq r \leq \tilde{m}_f.$$

Inserting (41) into (38) yields

$$\begin{aligned} u(t_{k+1}) = & u(t_k) + \lambda h^\alpha I_{h,m_u}^{\alpha,\sigma,p} u(t_{k+1}) + h^\alpha I_{h,m_f}^{\alpha,\delta,p} f(t_{k+1}, u(t_{k+1})) \\ & + h^\alpha \beta_0^{(p)} \left[-f(t_{k+1}, u(t_{k+1})) + E_k^p f(t_k, u(t_k)) \right] \end{aligned}$$

$$(45) \quad \begin{aligned} & + \sum_{j=1}^{\tilde{m}_f} W_{k,j}^{(\delta,p)} (f(t_j, u(t_j)) - f(0, u_0)) \Big] - \mathcal{H}_{\tilde{m}_u}^{\alpha,\sigma,p} u(t_{k+1}) \\ & + R_{k+1}^u + R_{k+1}^f + \tilde{R}_{k+1}^u + h^\alpha \beta_0^{(p)} \tilde{R}_{k+1}^f, \quad p = 0, 1. \end{aligned}$$

Finally, we obtain the IMEX(p) methods in the following form:

$$(46) \quad \begin{aligned} \frac{u_{k+1} - u_k}{h^\alpha} & = \lambda I_{h,m_u}^{\alpha,\sigma,p} u_{k+1} + I_{h,m_f}^{\alpha,\delta,p} f_{k+1} - \frac{1}{h^\alpha} \mathcal{H}_{\tilde{m}_u}^{\alpha,\sigma,p} u_{k+1} \\ & + \beta_0^{(p)} \left[-f_{k+1} + E_k^p f_k + \sum_{j=1}^{\tilde{m}_f} W_{k,j}^{(\delta,p)} (f_j - f_0) \right], \quad p = 0, 1, \end{aligned}$$

with $I_{h,m_u}^{\alpha,\sigma,p} u_{k+1}$, $\mathcal{H}_{\tilde{m}_u}^{\alpha,\sigma,p} u_{k+1}$, $I_{h,m_f}^{\alpha,\delta,p} f_{k+1}$ and $E_k^p f_k$ given, respectively, by (28), (29), (40) and

$$(47) \quad E_k^p f_k = \begin{cases} f_k, & p = 0, \\ 2f_k - f_{k-1}, & p = 1. \end{cases}$$

Remark 4. If $\alpha = 1$, the history load term for (30) is zero and we don't need to add the correction terms to solve (30). Moreover, (46) recovers the standard IMEX methods.

In the following, we will present the convergence results for the IMEX(p) methods (46). For this purpose, we first introduce some preparatory results. Both of the proofs will be given in Appendix B.

LEMMA 5. *The correction weights $W_{k,j}^{(\alpha,\sigma,p)}$, $\tilde{W}_{k,j}^{(\alpha,\sigma,p)}$, $W_{k,j}^{(\alpha,\delta,p)}$ and $W_{k,j}^{(\delta,p)}$ in (19), (22), (35) and (41), respectively, satisfy*

$$\begin{aligned} |W_{k,j}^{(\alpha,\sigma,p)}| & = \mathcal{O}((k+1)^{\sigma_{m_u} - p - 1}), & |W_{k,j}^{(\alpha,\delta,p)}| & = \mathcal{O}((k+1)^{\delta_{m_f} - p - 1}), \\ |\tilde{W}_{k,j}^{(\alpha,\sigma,p)}| & = \mathcal{O}((k+1)^{-\alpha - 1}) + \mathcal{O}((k+1)^{\sigma_{m_u} - p - 1}), & |W_{k,j}^{(\delta,p)}| & = \mathcal{O}((k+1)^{\delta_{\tilde{m}_f} - p - 1}). \end{aligned}$$

THEOREM 6. *Suppose that the Lipschitz condition (31) holds. If $\sigma_{\tilde{m}_u} \leq p + 1$, $\sigma_{m_u}, \delta_{m_f}, \delta_{\tilde{m}_f} \leq p + \alpha + 1$, then, for the IMEX(p) methods (46), there exists a constant $C_4 > 0$ independent of h such that*

$$(48) \quad \max_{0 \leq k \leq N} \|u(t_k) - u_k\|_\infty \leq C_4 \left(\sum_{j=1}^M \|u(t_j) - u_j\|_\infty + h^q \right),$$

where $M = \max \{m_u, m_f, \tilde{m}_u, \tilde{m}_f\}$ and

$$q = \min \{p + 1, \sigma_{\tilde{m}_u} + p, \sigma_{m_u} + \alpha + p, \delta_{m_f} + \alpha + p, \delta_{\tilde{m}_f} + \alpha + p\}.$$

3. Linear Stability of IMEX(p) Methods. In this section, we investigate the linear stability of the proposed IMEX(p) methods (46) by considering the following usual scalar test equation

$$(49) \quad {}^C D_t^\alpha u(t) = \lambda u(t) + \rho u(t), \quad \alpha \in (0, 1], \quad t \geq 0, \quad \lambda, \rho \in \mathbb{C}; \quad u(0) = u_0.$$

For this, the following result from [29] is useful to determine the stability regions of the obtained numerical schemes.

LEMMA 7. (cf. [29]) Assume that the sequence $\{g_k\}$ is convergent and that the quadrature weights $w_k (k \geq 1)$ satisfy

$$w_k = \frac{k^{\alpha-1}}{\Gamma(\alpha+1)} + v_k, \text{ where } \sum_{k=1}^{\infty} |v_k| < \infty,$$

then the stability region of the convolution quadrature $u_k = g_k + \hat{h} \sum_{j=0}^k w_{k-j} u_j$ is

$$S = \left\{ \hat{h} \in \mathbb{C} : 1 - \hat{h} w^\alpha(\xi) \neq 0, |\xi| \leq 1 \right\}, \text{ where } w^\alpha(\xi) = \sum_{j=0}^{\infty} w_j \xi^j,$$

where $\hat{h} = h^\alpha(\lambda + \rho)$ or \hat{h} is some function of $h^\alpha(\lambda + \rho)$.

We first consider the linear stability of the IMEX(0) for the test equation (49), it holds that

$$\begin{aligned} u_{k+1} &= u_k + \frac{\lambda h^\alpha}{\Gamma(\alpha+1)} u_{k+1} + h^\alpha \left(\lambda \sum_{j=1}^{m_u} W_{k,j}^{(\alpha,\sigma,0)} + \rho \sum_{j=1}^{m_f} W_{k,j}^{(\alpha,\delta,0)} \right) (u_j - u_0) \\ &\quad + \frac{\rho h^\alpha}{\Gamma(\alpha+1)} \left[u_k + \sum_{j=1}^{\tilde{m}_f} W_{k,j}^{(\delta,0)} (u_j - u_0) \right] - \frac{1}{\Gamma(\alpha)\Gamma(2-\alpha)} \sum_{j=0}^k \gamma_{k,j}^{(0)} u_j \\ &\quad - \sum_{j=1}^{\tilde{m}_u} \tilde{W}_{k,j}^{(\alpha,\sigma,0)} (u_j - u_0) \\ (50) \quad &= u_k + \frac{h^\alpha}{\Gamma(\alpha+1)} (\lambda u_{k+1} + \rho u_k) - \frac{1}{\Gamma(\alpha)\Gamma(2-\alpha)} \sum_{j=0}^k \gamma_{k,j}^{(0)} u_j + \sum_{j=1}^M W_{k,j} (u_j - u_0), \end{aligned}$$

where

$$\begin{aligned} \sum_{j=1}^M W_{k,j} (u_j - u_0) &= \lambda h^\alpha \sum_{j=1}^{m_u} W_{k,j}^{(\alpha,\sigma,0)} (u_j - u_0) + \rho h^\alpha \sum_{j=1}^{m_f} W_{k,j}^{(\alpha,\delta,0)} (u_j - u_0) \\ &\quad + \frac{\rho h^\alpha}{\Gamma(\alpha+1)} \sum_{j=1}^{\tilde{m}_f} W_{k,j}^{(\delta,0)} (u_j - u_0) - \sum_{j=1}^{\tilde{m}_u} \tilde{W}_{k,j}^{(\alpha,\sigma,0)} (u_j - u_0). \end{aligned}$$

Since $\sum_{j=1}^M W_{k,j} (u_j - u_0)$ does not affect the stability analysis, so we don't give the exact expression of $W_{k,j}$. Denote $U(\xi) = \sum_{k=0}^{\infty} u_k \xi^k$, $|\xi| \leq 1$. Then it follows from (50)

that

$$\begin{aligned} \sum_{k=0}^{\infty} u_{k+1} \xi^k &= \sum_{k=0}^{\infty} u_k \xi^k + \frac{\lambda h^\alpha}{\Gamma(\alpha+1)} \sum_{k=0}^{\infty} u_{k+1} \xi^k + \frac{\rho h^\alpha}{\Gamma(\alpha+1)} \sum_{k=0}^{\infty} u_k \xi^k \\ &\quad - \frac{1}{\Gamma(\alpha)\Gamma(2-\alpha)} \sum_{k=0}^{\infty} \left(\sum_{j=0}^k \gamma_{k,j}^{(0)} u_j \right) \xi^k + \sum_{k=0}^{\infty} \sum_{j=1}^M W_{k,j} (u_j - u_0) \xi^k, \end{aligned}$$

which leads to

$$(51) \quad \begin{aligned} \frac{1}{\xi}(U(\xi) - u_0) &= U(\xi) + \frac{\lambda h^\alpha}{\Gamma(\alpha+1)\xi}(U(\xi) - u_0) + \frac{\rho h^\alpha}{\Gamma(\alpha+1)}U(\xi) \\ &\quad - \frac{1}{\Gamma(\alpha)\Gamma(2-\alpha)}\gamma_k^{(0)}(\xi)U(\xi) + \sum_{k=1}^{\infty} \sum_{j=1}^M W_{k,j}(u_j - u_0)\xi^k, \end{aligned}$$

where $\gamma_k^{(0)}(\xi) = \sum_{j=0}^{\infty} \gamma_{k,j}^{(0)}\xi^j$. We simplify (51) as

$$\left[1 - \xi - \frac{\lambda h^\alpha}{\Gamma(\alpha+1)} - \frac{\rho h^\alpha}{\Gamma(\alpha+1)}\xi + \frac{1}{\Gamma(\alpha)\Gamma(2-\alpha)}\gamma_k^{(0)}(\xi)\xi \right] U(\xi) = H(\xi),$$

where

$$H(\xi) = \sum_{k=0}^{\infty} H_k \xi^k = \left[1 - \frac{\lambda h^\alpha}{\Gamma(\alpha+1)} \right] u_0 + \sum_{k=1}^{\infty} \sum_{j=1}^m W_{k,j}(u_j - u_0)\xi^{k+1}.$$

By using Lemma 5, when

$$\sigma_{m_u}, \delta_{m_f}, \delta_{\tilde{m}_f} < 1, \quad \sigma_{\tilde{m}_u} < \alpha + 1,$$

we can obtain that $\{H_k\}$ is a convergent sequence. Moreover, we know from Lemma 1 that $\sum_{j=0}^{\infty} |\gamma_{k,j}^{(0)}| < \infty$. Then it follows from Lemma 7 that method IMEX(0) is stable if

$$1 - \xi - \frac{\lambda h^\alpha}{\Gamma(\alpha+1)} - \frac{\rho h^\alpha}{\Gamma(\alpha+1)}\xi + \frac{1}{\Gamma(\alpha)\Gamma(2-\alpha)}\gamma_k^{(0)}(\xi)\xi \neq 0, \quad \forall |\xi| \leq 1.$$

Similarly, we can obtain the stability region of the method IMEX(1). Then we have the following theorem.

THEOREM 8. *Let $\rho = \kappa\lambda$ and $\hat{h} = \lambda h^\alpha$. Then for $\sigma_{m_u}, \delta_{m_f}, \delta_{\tilde{m}_f} < p + 1$, $\sigma_{\tilde{m}_u} < \alpha + p + 1$, we have the stability region of IMEX(0):*

$$S_0 = \mathbb{C} \setminus \left\{ \hat{h} : \hat{h} = \frac{\Gamma(\alpha+1)}{1+\kappa\xi} \left(1 - \xi + \frac{\gamma_k^{(0)}(\xi)\xi}{\Gamma(\alpha)\Gamma(2-\alpha)} \right), |\xi| \leq 1 \right\}.$$

and the stability region of IMEX(1):

$$S_1 = \mathbb{C} \setminus \left\{ \hat{h} : \hat{h} = \frac{\Gamma(\alpha+2)}{(1+\kappa)(\alpha\xi+1)-\kappa(\xi-1)^2} \left(1 - \xi + \frac{\gamma_k^{(1)}(\xi)\xi}{\Gamma(\alpha)\Gamma(2-\alpha)} \right), |\xi| \leq 1 \right\},$$

where $\gamma_k^{(1)}(\xi) = \sum_{j=0}^{\infty} \gamma_{k,j}^{(1)}\xi^j$.

In Figure 2 (a)-(c), we plot the stability regions of the method IMEX(0) with $\alpha = 0.2, 0.5, 0.8$ and $\rho = 0.5\lambda$, respectively. We also plot the stability regions of the method IMEX(1) with $\alpha = 0.2, 0.5, 0.8$ and $\rho = 0.5\lambda$ in Figure 2 (d). As the functions $\gamma_k^{(p)}(\xi) = \sum_{j=0}^{\infty} \gamma_{k,j}^{(p)}\xi^j$ is not explicitly known, so in all these figures we take $k = 10^5$.

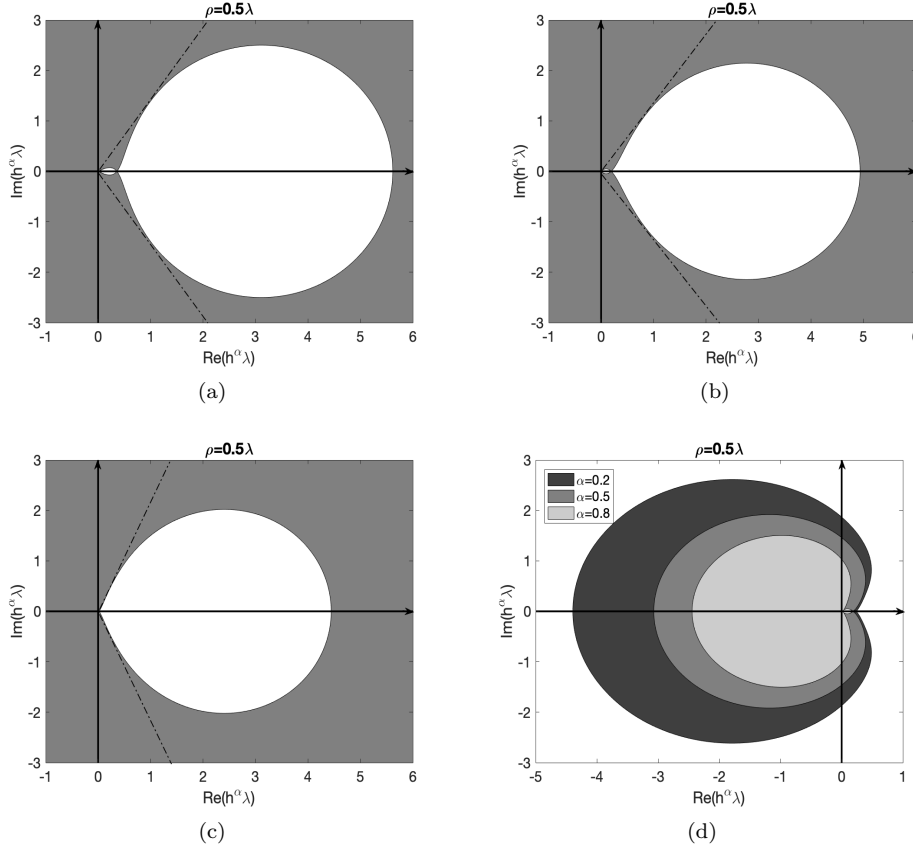


FIG. 2. (a) Stability region of $IMEX(0)$ with $\alpha = 0.2$ and $\rho = 0.5\lambda$; (b) Stability region of $IMEX(0)$ with $\alpha = 0.5$ and $\rho = 0.5\lambda$; (c) Stability region of $IMEX(0)$ with $\alpha = 0.8$ and $\rho = 0.5\lambda$; (d) Stability region of the $IMEX(1)$ with different α and $\rho = 0.5\lambda$.

4. The Fast Implementation of $IMEX(p)$ Methods. The step-by-step numerical solution of (46) for N time-steps requires $\mathcal{O}(N^2)$ evaluations of the time-dependent coefficients given by the hypergeometric functions, making the scheme expensive. Hence, we rewrite (46) as the matrices form, where the corresponding convolution matrices of coefficients have the Toeplitz structure and thus we leverage the use of FFTs to obtain the solution of the problem with complexity $\mathcal{O}(N \log N)$. For simplicity and objectivity, we demonstrate the procedure only for the $IMEX(0)$ scheme, for which we start by introducing the notations

$$U = (u_1, u_2, \dots, u_N)^T, \quad F(U) = (f_1, f_2, \dots, f_N)^T,$$

where U denotes the unknown solution vector. Then $IMEX(0)$ can be written in a compact form:

$$(52) \quad (A \otimes I_d - \lambda B \otimes I_d)U = h^\alpha (B \otimes I_d + C \otimes I_d)F(U) + D,$$

where \otimes denotes the Kronecker product and I_d represents the $d \times d$ identity matrix. Here the value of d can represent, for instance, the number of equations for a system

of nonlinear FDEs. Furthermore, we have:

$$(53) \quad A = \begin{bmatrix} 1 & & & & \\ -1 + \frac{\gamma_{1,1}^{(0)}}{\Gamma(\alpha)\Gamma(2-\alpha)} & 1 & & & \\ \frac{\gamma_{2,1}^{(0)}}{\Gamma(\alpha)\Gamma(2-\alpha)} & -1 + \frac{\gamma_{2,2}^{(0)}}{\Gamma(\alpha)\Gamma(2-\alpha)} & 1 & & \\ \vdots & \vdots & \ddots & \ddots & \\ \frac{\gamma_{N-1,1}^{(0)}}{\Gamma(\alpha)\Gamma(2-\alpha)} & \frac{\gamma_{N-1,2}^{(0)}}{\Gamma(\alpha)\Gamma(2-\alpha)} & \cdots & -1 + \frac{\gamma_{N-1,N-1}^{(0)}}{\Gamma(\alpha)\Gamma(2-\alpha)} & 1 \end{bmatrix} \in \mathbb{R}^{N \times N},$$

$$(54) \quad B = \frac{1}{\Gamma(\alpha+1)} I_N, \quad C = \frac{1}{\Gamma(\alpha+1)} \begin{bmatrix} -1 & & & & \\ 1 & -1 & & & \\ 0 & 1 & -1 & & \\ \vdots & \ddots & \ddots & \ddots & \\ 0 & \cdots & 0 & 1 & -1 \end{bmatrix} \in \mathbb{R}^{N \times N},$$

and D is a vector related to the corrections and solutions for the initial steps, in the following way:

$$(55) \quad \begin{aligned} D &= \lambda h^\alpha (W_{m_u} \otimes I_d) U_{m_u} + h^\alpha (W_{m_f} \otimes I_d) F(U_{m_f}) - (W_{\tilde{m}_u} \otimes I_d) U_{\tilde{m}_u} \\ &+ \frac{h^\alpha}{\Gamma(\alpha+1)} (W_{\tilde{m}_f} \otimes I_d) F(U_{\tilde{m}_f}) + (a_0 \otimes I_d) u_0 + h^\alpha (b_0 \otimes I_d) f_0, \end{aligned}$$

where the correction weights $W_{\hat{M}}$ ($\hat{M} = m_u, m_f, \tilde{m}_u, \tilde{m}_f$) are denoted by the $N \times \hat{M}$ matrices with the element $W_{k,j}^{(\alpha,\sigma,0)}$, $W_{k,j}^{(\alpha,\delta,0)}$, $\tilde{W}_{k,j}^{(\alpha,\sigma,0)}$ and $\tilde{W}_{k,j}^{(\delta,0)}$, respectively, for $k = 0, 1, \dots, N-1$ and $j = 1, 2, \dots, \hat{M}$. We also have,

$$\begin{aligned} a_0 &= \left(1, \frac{\gamma_{1,0}^{(0)}}{\Gamma(\alpha)\Gamma(2-\alpha)}, \frac{\gamma_{2,0}^{(0)}}{\Gamma(\alpha)\Gamma(2-\alpha)}, \dots, \frac{\gamma_{N-1,0}^{(0)}}{\Gamma(\alpha)\Gamma(2-\alpha)} \right)^T \in \mathbb{R}^N, \\ b_0 &= \left(\frac{1}{\Gamma(\alpha+1)}, 0, \dots, 0 \right)^T \in \mathbb{R}^N, \quad U_{\hat{M}} = (u_1 - u_0, u_2 - u_0, \dots, u_{\hat{M}} - u_0)^T. \end{aligned}$$

From (13), we observe that $\mathcal{A}_{k+1,j+1} = \mathcal{A}_{k,j}$, and therefore A is a lower-triangular Toeplitz matrix.

In what follows, we will analyze the unique solvability of the IMEX(0) scheme. For this purpose, we introduce the mapping $\Phi_h : \mathbb{R}^{N^d} \rightarrow \mathbb{R}^{N^d}$ as follows:

$$\Phi_h(X) := h^\alpha [(A - \lambda B)^{-1} (B + C) \otimes I_d] F(X) + [(A - \lambda B)^{-1} \otimes I_d] D,$$

and therefore, we have the following result.

THEOREM 9. *Suppose that Lipschitz condition (31) holds and*

$$(56) \quad h^\alpha L \|(A - \lambda B)^{-1} (B + C)\|_\infty < 1.$$

Then the method IMEX(0) has a unique solution $U \in \mathbb{R}^{N^d}$.

Proof. Let $X = (x_1^T, x_2^T, \dots, x_N^T)^T$, $\hat{X} = (\hat{x}_1^T, \hat{x}_2^T, \dots, \hat{x}_N^T)^T$ be two arbitrary vectors in \mathbb{R}^{Nd} . It follows from the Lipschitz condition (31) that

$$\begin{aligned} \left\| \Phi_h(X) - \Phi_h(\hat{X}) \right\|_\infty &\leq h^\alpha \left\| (A - \lambda B)^{-1}(B + C) \right\|_\infty \left\| F(X) - F(\hat{X}) \right\|_\infty \\ &\leq h^\alpha L \left\| (A - \lambda B)^{-1}(B + C) \right\|_\infty \left\| X - \hat{X} \right\|_\infty. \end{aligned}$$

If condition (56) holds, we know that $\Phi_h(X)$ is a contraction mapping with contraction factor $h^\alpha L \left\| (A - \lambda B)^{-1}(B + C) \right\|_\infty$. Moreover, it is well known that space \mathbb{R}^{Nd} with norm $\|\cdot\|_\infty$ is complete. Hence, according to the Banach contraction mapping principle (see e.g. [2]), mapping $\Phi_h(X)$ has a unique fixed point in \mathbb{R}^{Nd} . Namely, the method IMEX(0) has a unique solution $U \in \mathbb{R}^{Nd}$. \square

Remark 10. It should be pointed that, the coefficient matrices A for IMEX(1) is not the Toeplitz matrices, but we can choose the first column a_1 of A as

$$\hat{a}_1 = \left(1, -1 + \frac{\gamma_{2,2}^{(1)}}{\Gamma(\alpha)\Gamma(2-\alpha)}, \frac{\gamma_{3,2}^{(1)}}{\Gamma(\alpha)\Gamma(2-\alpha)}, \dots, \frac{\gamma_{N,2}^{(1)}}{\Gamma(\alpha)\Gamma(2-\alpha)} \right)^T \in \mathbb{R}^N.$$

Then A will be a Toeplitz matrix. Moreover, if we do this, the corresponding vector D for IMEX(1) will be change by adding the term $[(\hat{a}_1 - a_1) \otimes I_d] U$.

4.1. Fast Approximate Inversion Scheme. In order to obtain a fast solution to the Toeplitz system (52), we employ the scheme developed in [26], which approximates the lower-triangular Toeplitz matrix K^{-1} . In particular, we have $K = (A \otimes I_d - \lambda B \otimes I_d)$ for the method IMEX(0) in (52). The first step involves approximating the matrix K by the following block ϵ -circulant matrix:

$$(57) \quad K_\epsilon = \begin{bmatrix} K_0 & \epsilon K_{N-1} & \dots & \epsilon K_2 & \epsilon K_1 \\ K_1 & K_0 & \epsilon K_{N-1} & \dots & \epsilon K_2 \\ \vdots & K_1 & K_0 & \ddots & \vdots \\ K_{N-2} & \dots & \ddots & \ddots & \epsilon K_{N-1} \\ K_{N-1} & K_{N-2} & \dots & K_1 & K_0 \end{bmatrix},$$

with $\epsilon > 0$. It is reported by Lu *et al.* [26] that the accuracy of the fast inversion is $\mathcal{O}(\epsilon)$, where mathematically ϵ can be taken arbitrarily small. However, for double-precision arithmetic, ϵ cannot be set too small due to rounding errors. Numerical experiments demonstrated the smallest practical value to be $\epsilon = 5 \times 10^{-9}$. It is also shown in [26] that K_ϵ^{-1} is also a block ϵ -circulant matrix, and therefore the solution to system (52) can be written in the following way:

$$U \approx K_\epsilon^{-1} R,$$

where R denote the right-hand side of (52).

Let $D_\varrho = \text{diag}(1, \varrho, \dots, \varrho^{N-1})$, with $\varrho = \epsilon^{1/N}$ be a diagonal matrix and F_N be a $N \times N$ Fourier matrix. We then have the following spectral decomposition:

$$K_\epsilon^{-1} = [(D_\varrho^{-1} F_N^*) \otimes I_d] \text{diag}(\Lambda_0^{-1}, \Lambda_1^{-1}, \dots, \Lambda_{N-1}^{-1}) [(F_N D_\varrho) \otimes I_d],$$

with

$$(58) \quad \begin{bmatrix} \Lambda_0 \\ \Lambda_1 \\ \vdots \\ \Lambda_{N-1} \end{bmatrix} = [(\sqrt{N}F_N D_\varrho) \otimes I_d] \begin{bmatrix} K_0 \\ K_1 \\ \vdots \\ K_{N-1} \end{bmatrix}.$$

Finally, the approximate solution for U becomes:

$$(59) \quad U \approx [(D_\varrho^{-1} F_N^* \otimes I_d) \text{diag}(\Lambda_0^{-1}, \Lambda_1^{-1}, \dots, \Lambda_{N-1}^{-1}) [(F_N D_\varrho) \otimes I_d] R,$$

where in practical implementations, we replace the Fourier matrices F_N in (58) and (59) with FFT operations in order to achieve a computational complexity of $\mathcal{O}(N \log N)$. The other operations to form R do not require FFTs, since matrices B and C are sparse, lower-Toeplitz nature, and the vector D is formed through the multiplication of tall matrices with small vectors.

Remark 11. Note that (59) is a nonlinear system, therefore iterative solver should be applied to solve this problem. As is known, the Newton iteration method may be the most popular solver for a general system of nonlinear equations $G(x) = 0$. However, the disadvantages of the Newton iteration method is that, at each iteration step, it requires the explicit form of the $N \times N$ Jacobian matrix $G'(x^{(n)})$, where $x^{(n)}$ denotes the n th-approximation to x . So the computation of the Newton iteration method could be much more expensive. In order to overcome this disadvantage, Picard iteration method has been used to solve the system (59), where, for a given iteration n , we have:

$$(60) \quad U^{(n+1)} = K_\epsilon^{-1} R(U^{(n)}),$$

until $\|U^{(n+1)} - U^{(n)}\| > \epsilon^p$, where $U^{(n)}$ denotes the n th-approximation to U and ϵ^p represents the tolerance of the Picard iteration scheme.

4.2. Fast Computation of Hypergeometric Functions. Accurate and efficient computations of the Gauss hypergeometric function ${}_2F_1(a, b; c; z)$ is also fundamental to the developed scheme. From [35], we know that there is no simple answer for this problem, and different methods are optimal for different parameter regimes. When $\Re(c) > \Re(a) > 0$ or $\Re(c) > \Re(b) > 0$, the Gauss-Jacobi quadrature method is effective. As stated in [1], when $|\arg(1-z)| < \pi$, we have

$$(61) \quad {}_2F_1(a, b; c; z) = \frac{\Gamma(c)}{\Gamma(b)\Gamma(c-b)} \int_0^1 (1-zt)^{-a} w_{b,c}(t) dt, \quad \Re(c) > \Re(b) > 0,$$

where $w_{b,c}(t) = (1-t)^{c-b-1} t^{b-1}$. The parameters a and b in (61) can be interchanged due to the basic power series definition of the hypergeometric function. Transforming $t \rightarrow \frac{\tilde{t}+1}{2}$, we can obtain that

$$\begin{aligned} \int_0^1 (1-zt)^{-a} w_{b,c}(t) dt &= \frac{1}{2^{c-1}} \int_{-1}^1 \left(1 - \frac{1}{2}z - \frac{1}{2}z\tilde{t}\right)^{-a} (1-\tilde{t})^{c-b-1} (1+\tilde{t})^{b-1} dt \\ &= \sum_{j=1}^Q w_j^{GJ} \left(1 - \frac{1}{2}z - \frac{1}{2}z t_j^{GJ}\right)^{-a} + E_Q(a, b, z), \end{aligned}$$

where t_j^{GJ} and w_j^{GJ} are the Gauss-Jacobi nodes and weights on $[-1, 1]$, and Q is the number of mesh points. Error bounds for this method are discussed in [17].

4.3. Algorithm of IMEX(p) Methods. We present the main stages of the developed fast IMEX(p) methods for efficient time-integration of nonlinear FDEs in Algorithm I. The algorithm particularly described the IMEX(0) approach, but the main steps remain the same for IMEX(1), with slight modifications regarding the number of sets of correction weights and forms for the nonlinear system matrices. The operators $\mathcal{F}(\cdot)$ and $\mathcal{F}^{-1}(\cdot)$ represent, respectively, the forward and inverse Fast Fourier Transforms.

Algorithm I Fast IMEX(0) Integration Scheme for Nonlinear FDEs.

- 1: **Known database:**
 - 2: Initial parameters $h, N, \epsilon, \epsilon^p, \lambda$, number of correction terms and powers σ, δ .
 - 3: Compute the first column a_1 of A defined in (53). Compute B and C defined in (54) with sparse allocation.
 - 4: Compute corrections using (20)-(21), (25), (36)-(37) and (43) (or (44)) for all N time-steps.
 - 5: Compute D_ρ . Assemble the first column $K_{\epsilon,1}$ of K_ϵ in (57).
 - 6: Compute $\Lambda = \mathcal{F}((D_\rho \otimes I_d)K_{\epsilon,1})$ to obtain (58).
 - 7: **Picard Iteration:** Initial guess $U^{(0)}$.
 - 8: **while** $e > \epsilon^p$ **do**
 - 9: Compute $D(U^{(n)})$ using (55). Compute $F(U^{(n)})$.
 - 10: Compute $R(U^{(n)})$ using (52)
 - 11: Compute $r_\epsilon = \mathcal{F}((D_\rho \otimes I_d)R(U^{(n)}))$
 - 12: Solve $\tilde{r}_\epsilon = \Lambda^{-1}r_\epsilon$
 - 13: Compute the updated solution vector $U^{(n+1)} = D_\rho^{-1}\mathcal{F}^{-1}(\tilde{r}_\epsilon)$.
 - 14: Compute $e = \|U^{(n+1)} - U^{(n)}\|$.
 - 15: $n = n + 1$
 - 16: **end while**
 - 17: **return** $U^{(n+1)}$
-

Remark 12. For the FAMMs (17), (33) and the FAMMs with correction terms (27), (39), we also can use the fast implementation proposed in this section to construct the corresponding fast methods.

5. Numerical Tests. We present several numerical examples to verify our theoretical analysis presented in the previous sections. In all presented numerical examples, we utilize a numerical tolerance $\epsilon = 5 \times 10^{-9}$ for the fast inversion step. For all hypergeometric functions involved in the evaluation of correction weights and history load term, we utilize $Q = 200$ Gauss-Jacobi quadrature points. One exception is the incomplete beta function evaluated for the history load correction in (25). For this case, the argument $\frac{k}{k+1}$ approaches 1 as N increases, and a numerical quadrature becomes a poor choice due to singularities. In that sense we evaluate the incomplete beta function using the native MATLAB implementation. Furthermore, given $\Omega = (0, T]$, we utilize the following quantities:

$$\text{err}_N(h) = \frac{\|u(t_N) - u_N\|_\infty}{\|u(t_N)\|_\infty}, \quad \text{err}(h) = \frac{\max_{0 \leq k \leq N} \|u(t_k) - u_k\|_\infty}{\max_{0 \leq k \leq N} \|u(t_k)\|_\infty},$$

$$\text{Order}_1 = \log_2 \left[\frac{\text{err}_N(h)}{\text{err}_N(h/2)} \right], \quad \text{Order}_2 = \log_2 \left[\frac{\text{err}(h)}{\text{err}(h/2)} \right]$$

to denote the error at the endpoint T , the global error on the solution interval Ω and convergence order of the used method at the endpoint T and on the solution interval Ω , respectively. The developed framework was implemented in MATLAB R2019a and was run in a desktop computer with Intel Core i7-6700 CPU with 3.40 GHz, 16 GB RAM and Ubuntu 18.04.2 LTS operating system.

Example 13. Linear FDE (see e.g. [57]):

$$(62) \quad {}_0^C D_t^\alpha u(t) = f(t), \quad \alpha \in (0, 1], \quad t \in (0, 1]; \quad u(0) = 0.$$

The exact solution of (62) is $u(t) = t^{p+\alpha}$ for $p = 1, 2$. Therefore the corresponding force term is $f(t) = \frac{\Gamma(\alpha+p+1)}{\Gamma(p+1)} t^p$. Recalling Remark 12, we can employ the fast inversion scheme directly to the FAMM (17) in order to obtain a fast FAMM. Therefore, in this example we compare the performance between the fast and original FAMMs (17), where we verify the computational complexity and accuracy of both original and fast schemes.

Table 1 presents the obtained results for the implemented FAMMs and at the endpoint $T = 1$. Similar to the results in [57], we observe that the convergence order is independent of the fractional order α , preserving the accuracy of the integer-order methods. The computational times for the original and fast FAMMs are illustrated in Figure 3. We observe the computational complexity of $\mathcal{O}(N \log N)$ for the developed fast FAMMs. Since no break-even point is observed between both methods, the fast method is more computationally efficient regardless of the value of N .

TABLE 1

The errors at the endpoint and convergence orders of the FAMMs for (62) with $p = 0$ (upper table) and $p = 1$ (lower table).

The fast FAMM with $p = 0$.						
h	$\alpha = 0.1$		$\alpha = 0.5$		$\alpha = 0.9$	
	$\text{err}_N(h)$	Order ₁	$\text{err}_N(h)$	Order ₁	$\text{err}_N(h)$	Order ₁
2^{-3}	5.2795e-03	–	9.7878e-03	–	1.0461e-03	–
2^{-4}	2.6031e-03	1.0202	5.0535e-03	0.9537	6.0576e-04	0.7883
2^{-5}	1.2912e-03	1.0115	2.5658e-03	0.9779	3.3733e-04	0.8446
2^{-6}	6.4272e-04	1.0064	1.2925e-03	0.9892	1.8357e-04	0.8778
2^{-7}	3.2058e-04	1.0035	6.4866e-04	0.9947	9.8414e-05	0.8994

The fast FAMM with $p = 1$.						
h	$\alpha = 0.1$		$\alpha = 0.5$		$\alpha = 0.9$	
	$\text{err}_N(h)$	Order ₁	$\text{err}_N(h)$	Order ₁	$\text{err}_N(h)$	Order ₁
2^{-3}	2.1934e-05	–	4.0975e-04	–	4.9840e-04	–
2^{-4}	5.5334e-06	1.9869	9.6888e-05	2.0804	1.2210e-04	2.0292
2^{-5}	1.4102e-06	1.9723	2.3574e-05	2.0391	2.9761e-05	2.0366
2^{-6}	3.5857e-07	1.9756	5.8150e-06	2.0193	7.2452e-06	2.0383
2^{-7}	8.9586e-08	2.0009	1.4452e-06	2.0085	1.7663e-06	2.0363

Example 14. Stiff FDE (see e.g. [6]):

$$(63) \quad {}_0^C D_t^\alpha u(t) = Pu(t) + Su(t) + g(t), \quad \alpha \in (0, 1], \quad t \in (0, 10]; \quad u(0) = [1, 1, 1]^T,$$

where

$$P = \begin{bmatrix} -1 & 0 & 0.001 \\ -0.0005 & -0.0008 & -0.0002 \\ 0.001 & 0 & -0.001 \end{bmatrix}, \quad S = \begin{bmatrix} -0.006 & 0 & 0.002 \\ -0.001 & -0.002 & 0 \\ 0 & -0.005 & -0.008 \end{bmatrix},$$

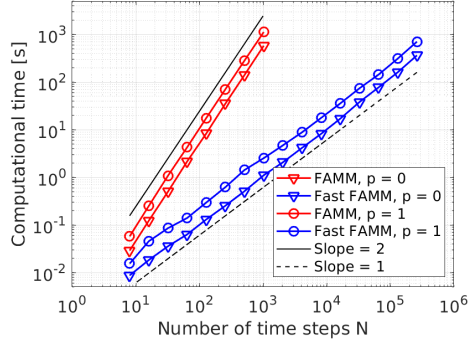


FIG. 3. Computational time versus number of time steps N for the original (red curves) and the developed, fast (blue curves) FAMMs.

$$g(t) = \begin{pmatrix} a_1 \Gamma_1 t^{\sigma_1 - \alpha} + a_2 \Gamma_2 t^{\sigma_2 - \alpha} \\ a_3 \Gamma_3 t^{\sigma_3 - \alpha} + a_4 \Gamma_4 t^{\sigma_4 - \alpha} \\ a_5 \Gamma_5 t^{\sigma_5 - \alpha} + a_6 \Gamma_6 t^{\sigma_6 - \alpha} \end{pmatrix} - (P + S) \begin{pmatrix} a_1 t^{\sigma_1} + a_2 t^{\sigma_2} + 1 \\ a_3 t^{\sigma_3} + a_4 t^{\sigma_4} + 1 \\ a_5 t^{\sigma_5} + a_6 t^{\sigma_6} + 1 \end{pmatrix},$$

with $\Gamma_k = \frac{\Gamma(\sigma_k + 1)}{\Gamma(\sigma_k + 1 - \beta)}$, $1 \leq k \leq 6$. Therefore, the exact solution for the stiff FDE (63) is given by:

$$u(t) = (a_1 t^{\sigma_1} + a_2 t^{\sigma_2} + 1, a_3 t^{\sigma_3} + a_4 t^{\sigma_4} + 1, a_5 t^{\sigma_5} + a_6 t^{\sigma_6} + 1)^T,$$

where, as in [6], we consider $\sigma_1 = \alpha$, $\sigma_2 = 2\alpha$, $\sigma_3 = 1 + \alpha$, $\sigma_4 = 5\alpha$, $\sigma_5 = 2$, $\sigma_6 = 2 + \alpha$, and $a_1 = 0.5$, $a_2 = 0.8$, and $a_3 = a_4 = a_5 = a_6 = 1$. For the numerical solution of (63), we take $f(t, u) = Su(t) + g(t)$ and employ the IMEX(p) scheme with $\alpha = 0.3$, utilizing a Picard iteration tolerance of $\epsilon^p = 5 \times 10^{-7}$. We remark that the coefficients of P and S are taken as small enough values in order to satisfy the Lipschitz condition for the Picard iteration scheme, and nevertheless, the choice of such values still makes (63) stiff. The obtained results are presented in Table 2, where we obtain first-order convergence for the IMEX(0) method without using correction terms. On the other hand, for IMEX(1), we obtain second-order convergence when using $M = 3$ correction terms with correction powers $\sigma = \{\alpha, 2\alpha, 1 + \alpha\}$ and $\delta = \{2\alpha, 1 + \alpha, 5\alpha\}$.

Example 15. Nonlinear FDE (cf. [6, 60]):

$$(64) \quad {}_0^C D_t^\alpha u(t) = \lambda u(t) + f(t, u(t)), \quad \alpha \in (0, 1], \quad t \in \Omega; \quad u(0) = u_0.$$

We consider the following cases for (64):

- **Case I)** Let $\lambda = -0.2$, $f(t, u(t)) = 0$ and $u_0 = 1$. The corresponding analytical solution is given by $u(t) = E_\alpha(-0.2t^\alpha)$, where $E_\alpha(t)$ represents the Mittag-Leffler function (cf. [31]).
- **Case II)** Let $\lambda = -1$, $f(t, u(t)) = -0.1u^2 + g(t)$, $u_0 = 1$ and choose $g(t)$ such that the exact solution of (64) is given by $u(t) = 1 + t + t^2/2 + t^3/3 + 4^4/4$.
- **Case III)** Let $\lambda = -1$, $f(t, u(t)) = 0.01u(1 - u^2) + 2 \cos(2\pi t)$ and $u_0 = 1$.

We start with **Case I)**, for which we consider $\Omega = (0, 40]$ and a tolerance $\epsilon^p = 10^{-7}$ for the Picard iteration, with varying number of correction terms M and $\alpha = 0.4$. The obtained results are presented in Table 3 for the methods IMEX(p), where the

TABLE 2

The global errors and convergence orders of the methods $IMEX(p)$ for (63) with $p = 0$ (upper table) and $p = 1$ (lower table) and $\alpha = 0.3$.

IMEX(0)								
h	$M = 0$			$M = 1$				
	err(h)	Order ₂		err(h)	Order ₂			
2^{-3}	1.9340e-02	–		1.9271e-02	–			
2^{-4}	9.7036e-03	0.9950		9.6793e-03	0.9935			
2^{-5}	4.8614e-03	0.9972		4.8518e-03	0.9964			
2^{-6}	2.4334e-03	0.9984		2.4294e-03	0.9979			
2^{-7}	1.2175e-03	0.9991		1.2157e-03	0.9988			

IMEX(1)								
h	$M = 0$		$M = 1$		$M = 2$		$M = 3$	
	err(h)	Order ₂	err(h)	Order ₂	err(h)	Order ₂	err(h)	Order ₂
2^{-3}	6.5717e-04	–	4.3931e-04	–	2.4945e-04	–	2.1176e-04	–
2^{-4}	3.8296e-04	0.7791	1.5083e-04	1.5424	6.2702e-05	1.9922	5.6167e-05	1.9146
2^{-5}	2.3992e-04	0.6746	5.5600e-05	1.4397	1.5730e-05	1.9950	1.4606e-05	1.9431
2^{-6}	1.5407e-04	0.6390	2.1541e-05	1.3680	4.0658e-06	1.9519	3.7593e-06	1.9581
2^{-7}	9.9312e-05	0.6335	8.5481e-06	1.3334	1.7074e-06	1.2517	9.6316e-07	1.9646

CPU time (CPU) measured in seconds represent the running time of the methods. We observe the linear convergence rate when using $M = 2$ correction terms for $IMEX(0)$. The convergence rates also improve for $IMEX(1)$, however, we attain the accuracy limit of the scheme when using $M = 4$. Such accuracy limit is determined by the value of $\epsilon = 5 \times 10^{-9}$ utilized for the fast inversion approach discussed in Section 4.1.

TABLE 3

The global errors and convergence orders of the methods $IMEX(p)$ for solving Case I) with $\alpha = 0.4$, varying h and correction terms M with corresponding powers $\sigma_k = \delta_k = k\alpha$.

h	M	IMEX(0)			M	IMEX(1)		
		err(h)	Order ₂	CPU		err(h)	Order ₂	CPU
2^{-2}		7.6111e-03	–	0.21		5.9001e-03	–	0.37
2^{-3}		5.7608e-03	0.4019	0.37		4.6835e-03	0.3352	0.68
2^{-4}	0	4.3450e-03	0.4069	0.75	0	3.6810e-03	0.3475	1.37
2^{-5}		3.2724e-03	0.4090	1.35		2.8698e-03	0.3591	2.65
2^{-6}		2.4640e-03	0.4093	2.65		2.2231e-03	0.3684	5.32
2^{-2}		1.9406e-03	–	0.22		2.1673e-05	–	1.06
2^{-3}		1.2144e-03	0.6762	0.35		1.0252e-05	1.0800	2.13
2^{-4}	1	7.4541e-04	0.7042	0.73	2	4.7644e-06	1.1055	4.03
2^{-5}		4.5062e-04	0.7261	1.36		2.1831e-06	1.1259	7.95
2^{-6}		2.6918e-04	0.7433	2.66		9.8961e-07	1.1415	16.04
2^{-2}		3.2061e-04	–	0.56		1.4155e-07	–	1.74
2^{-3}		1.7125e-04	0.9047	1.10		5.0125e-08	1.4978	3.32
2^{-4}	2	9.0232e-05	0.9244	1.97	4	2.5470e-08	0.9767	6.49
2^{-5}		4.7019e-05	0.9404	3.91		2.7468e-08	–	13.07
2^{-6}		2.4284e-05	0.9532	7.85		3.6517e-08	–	26.02

For **Case II**), we let $\Omega = (0, 1]$ and $\epsilon^p = 10^{-7}$. The obtained results are presented in Table 4, where we observe that both schemes achieve the theoretical convergence rates for the global error.

For **Case III**), we consider $\Omega = (0, 50]$, and we set a numerical tolerance $\epsilon^p =$

TABLE 4

The global errors and convergence orders of the methods IMEX(p) for solving Case II) with no correction term for $p = 0$ and $M = 2$ correction terms for $p = 1$, with $\sigma = \delta = \{1 - \alpha, 1\}$.

IMEX(0)						
h	$\alpha = 0.2$		$\alpha = 0.5$		$\alpha = 0.8$	
	err(h)	Order ₂	err(h)	Order ₂	err(h)	Order ₂
2^{-6}	1.9855e-02	–	1.8557e-02	–	1.7421e-02	–
2^{-7}	9.9111e-03	1.0024	9.2800e-03	0.9998	8.7136e-03	0.9994
2^{-8}	4.9517e-03	1.0011	4.6425e-03	0.9992	4.3602e-03	0.9989
2^{-9}	2.4750e-03	1.0005	2.3226e-03	0.9991	2.1821e-03	0.9987
2^{-10}	1.2373e-03	1.0002	1.1619e-03	0.9992	1.0921e-03	0.9986

IMEX(1)						
h	$\alpha = 0.2$		$\alpha = 0.5$		$\alpha = 0.8$	
	err(h)	Order ₂	err(h)	Order ₂	err(h)	Order ₂
2^{-6}	5.3875e-04	–	4.4167e-04	–	3.7370e-04	–
2^{-7}	1.3610e-04	1.9849	1.1153e-04	1.9856	9.4359e-05	1.9856
2^{-8}	3.4206e-05	1.9924	2.8033e-05	1.9922	2.3740e-05	1.9909
2^{-9}	8.5751e-06	1.9960	7.0286e-06	1.9958	5.9679e-06	1.9920
2^{-10}	2.1498e-06	1.9960	1.7586e-06	1.9988	1.4862e-06	2.0056

10^{-6} for the Picard iteration. Figures 4 and 5(a) illustrate the obtained highly oscillatory solutions. We also perform a convergence analysis utilizing a benchmark solution with $h = 2^{-11}$ and $M = 3$ correction terms and evaluate the global error. The obtained results are presented in Table 5, where the expected first- and second-order convergence rates are obtained, respectively, with $p = 0$ without correction terms, and $p = 1$ using $M = 3$ correction terms. The computational times for the developed IMEX schemes are illustrated in Figure 5(b) including the initial phase for computation of correction weights. We observe the computational complexity of $\mathcal{O}(N \log N)$ for the developed schemes even for nonlinear problems, with a small difference between the first- and second-order schemes.

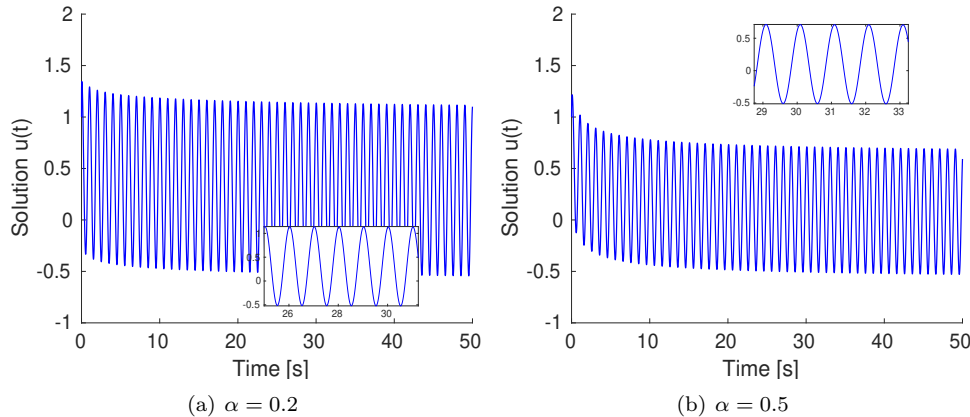


FIG. 4. Solution versus time t for Case III) using $h = 0.005$ and $M = 1$ correction term.

6. Conclusions. We developed two new first- and second-order IMEX schemes for accurate and efficient solution of stiff/nonlinear FDEs with singularities. Both

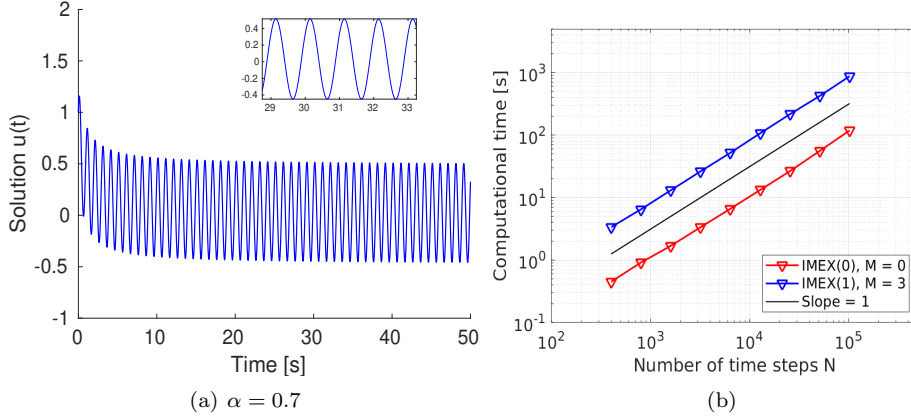


FIG. 5. (a) Solution versus time t for Case III) using $h = 0.005$ with $M = 1$ correction term. (b) Computational time versus number of time steps N for the developed IMEX schemes.

TABLE 5

Convergence results for the IMEX(p) scheme solving Case III) without corrections for $p = 0$ and $M = 3$ correction terms for $p = 1$, with $\sigma = \delta = \{\alpha, 2\alpha, 1 + \alpha\}$.

IMEX(0)						
h	$\alpha = 0.2$		$\alpha = 0.5$		$\alpha = 0.7$	
	err(h)	Order ₂	err(h)	Order ₂	err(h)	Order ₂
2^{-3}	4.4883e-01	–	3.3552e-01	–	2.5798e-01	–
2^{-4}	2.2466e-01	0.9984	1.6681e-01	1.0082	1.3311e-01	0.9546
2^{-5}	1.1217e-01	1.0021	8.3553e-02	0.9975	6.7629e-02	0.9769
2^{-6}	5.6354e-02	0.9931	4.2141e-02	0.9875	3.4015e-02	0.9915
2^{-7}	2.8246e-02	0.9965	2.1163e-02	0.9937	1.7091e-02	0.9929

IMEX(1)						
h	$\alpha = 0.2$		$\alpha = 0.5$		$\alpha = 0.7$	
	err(h)	Order ₂	err(h)	Order ₂	err(h)	Order ₂
2^{-3}	3.3534e-01	–	1.9664e-01	–	2.5260e-01	–
2^{-4}	9.5452e-02	1.8128	8.1541e-02	1.2699	7.1427e-02	1.8223
2^{-5}	2.2387e-02	2.0921	2.0062e-02	2.0230	2.0503e-02	1.8007
2^{-6}	5.4892e-03	2.0280	4.5814e-03	2.1306	4.8812e-03	2.0705
2^{-7}	1.8634e-03	1.5586	1.0402e-03	2.1389	1.1154e-03	2.1296

of the schemes are based on the linear multi-step FAMM developed by Zayernouri and Matzavinos [57], followed by an extrapolation formula from which we obtain the so-called IMEX(p) scheme. In order to handle the inherent singularities of the FDEs, we introduced 4 sets of correction terms for the IMEX(p) schemes. The convergence and linear stability of the developed schemes is also analyzed. A fast solution for the developed schemes is attained by employing a fast-inversion approach developed by Lu *et al.* [26] on the resulting nonlinear Toeplitz system, leading to a computational complexity of $\mathcal{O}(N \log N)$. Based on our computational results, we observed that:

- When considering a linear problem, the fast implementation of the scheme was significantly faster than the original FAMM by Zayernouri and Matzavinos [57], without even the presence of a *break-even* point.
- Both IMEX(p) schemes achieved global first- (for $p = 0$) and second-order (for

$p = 1$) convergence rates for stiff/nonlinear, highly-oscillatory and singular solutions, given the choice of appropriate sets of correction terms.

- The computational performance was slightly better for the IMEX(0) scheme. We also remark that such scheme is simpler to implement and generally requires a smaller number of correction terms due to lower regularity requirements to attain first-order accuracy.

The main advantages of the developed IMEX schemes in comparison to other works are: larger stability regions when compared to the IMEX schemes developed by Cao *et al.* [6]; and also a fast solution alternative when compared to the original fractional Adams-Bashforth/Moulton methods developed by Zayernouri and Matzavinos [57], and the IMEX schemes by Cao *et al.* [6]. When compared to the matrix-based fast solver for FDEs developed by Lu [26], the developed framework in this work handles the numerical solution of nonlinear and singular FDEs instead of only linear ones.

The developed schemes could be used for, *e.g.*, fractional visco-elastic models under complex loading conditions and long-time integration [19]. Regarding additional constitutive effects, such as fractional visco-elasto-plastic models [44, 48], and plasticity-driven damage formulations [46], the developed methods could be potentially applied under simple monotone loads. Furthermore, the introduction of additional sets of correction terms motivates the use of data-infused self-singularity-capturing approaches [47], which would decrease the number of correction terms per set.

Appendix A. Discretization Coefficients for the History Load Term.

We present the coefficients $\gamma_{k,j}^{(p)}$ ($0 \leq j \leq k$, $0 \leq k \leq N$, $p = 0, 1$) defined in (16):

$$\gamma_{0,0}^{(0)} = 0, \quad \gamma_{0,0}^{(1)} = 0, \quad \gamma_{1,0}^{(1)} = \frac{\mathcal{A}_{1,1} - \mathcal{A}_{1,0}}{h},$$

$$\gamma_{1,1}^{(1)} = \frac{\mathcal{A}_{1,0} - \mathcal{A}_{1,1}}{h}, \quad \gamma_{2,0}^{(1)} = \frac{-2\mathcal{A}_{2,0} + \mathcal{A}_{2,1} - \mathcal{A}_{2,2}}{2h} + \frac{\mathcal{B}_{2,1} - \mathcal{B}_{2,2}}{(2 - \alpha)h^2},$$

$$\gamma_{2,1}^{(1)} = \frac{\mathcal{A}_{2,0} - \mathcal{A}_{2,1} + 2\mathcal{A}_{2,2}}{h} - \frac{2\mathcal{B}_{2,1} - 2\mathcal{B}_{2,2}}{(2 - \alpha)h^2}, \quad \gamma_{2,2}^{(1)} = \frac{\mathcal{A}_{2,1} - 3\mathcal{A}_{2,2}}{2h} + \frac{\mathcal{B}_{2,1} - \mathcal{B}_{2,2}}{(2 - \alpha)h^2},$$

for $k \geq 1$,

$$\gamma_{k,j}^{(0)} = \begin{cases} \frac{\mathcal{A}_{k,1} - \mathcal{A}_{k,0}}{h}, & j = 0, \\ \frac{\mathcal{A}_{k,j-1} - 2\mathcal{A}_{k,j} + \mathcal{A}_{k,j+1}}{h}, & 1 \leq j \leq k-1, \\ \frac{\mathcal{A}_{k,k-1} - \mathcal{A}_{k,k}}{h}, & j = k, \end{cases}$$

and, for $k \geq 3$,

$$\gamma_{k,j}^{(1)} = \begin{cases} \frac{-2\mathcal{A}_{k,0} + \mathcal{A}_{k,1} - \mathcal{A}_{k,2} + \frac{\mathcal{B}_{k,1} - \mathcal{B}_{k,2}}{(2-\alpha)h^2}}{2h}, & j = 0, \\ \frac{2\mathcal{A}_{k,0} - 2\mathcal{A}_{k,1} + 3\mathcal{A}_{k,2} - \mathcal{A}_{k,3} + \frac{-2\mathcal{B}_{k,1} + 3\mathcal{B}_{k,2} - \mathcal{B}_{k,3}}{(2-\alpha)h^2}}{2h}, & j = 1, \\ \frac{\mathcal{A}_{k,j-1} - 3\mathcal{A}_{k,j} + 3\mathcal{A}_{k,j+1} - \mathcal{A}_{k,j+2}}{2h} \\ + \frac{\mathcal{B}_{k,j-1} - 3\mathcal{B}_{k,j} + 3\mathcal{B}_{k,j+1} - \mathcal{B}_{k,j+2}}{(2-\alpha)h^2}, & 2 \leq j \leq k-2, \\ \frac{\mathcal{A}_{k,k-2} - 3\mathcal{A}_{k,k-1} + 4\mathcal{A}_{k,k} + \frac{\mathcal{B}_{k,k-2} - 3\mathcal{B}_{k,k-1} + 2\mathcal{B}_{k,k}}{(2-\alpha)h^2}}{2h}, & j = k-1, \\ \frac{\mathcal{A}_{k,k-1} - 3\mathcal{A}_{k,k} + \frac{\mathcal{B}_{k,k-1} - \mathcal{B}_{k,k}}{(2-\alpha)h^2}}{2h}, & j = k. \end{cases}$$

Appendix B. Proofs.

B.1. Proof of Lemma 1. Before proof of Lemma 1, we need some preparatory results by introducing the notations:

$$(65) \quad a_l^{(\alpha)} = (l + \theta + 1)^{1-\alpha} - (l + \theta)^{1-\alpha}, \quad l \geq 0,$$

$$(66) \quad b_l^{(\alpha)} = \frac{(l + \theta + 1)^{2-\alpha} - (l + \theta)^{2-\alpha}}{2 - \alpha} - \frac{(l + \theta + 1)^{1-\alpha} + (l + \theta)^{1-\alpha}}{2}, \quad l \geq 0,$$

and

$$(67) \quad c_l^{(\alpha)} = \begin{cases} a_0^{(\alpha)} + b_0^{(\alpha)}, & l = 0, \\ a_l^{(\alpha)} + b_l^{(\alpha)} - b_{l-1}^{(\alpha)}, & 1 \leq l \leq k-2, \\ a_l^{(\alpha)} - b_{l-1}^{(\alpha)}, & l = k-1. \end{cases}$$

where $\theta \in [0, 1]$. The following lemma states the properties of the above defined notations.

LEMMA 16. For any α ($0 < \alpha \leq 1$) and $\{a_l^{(\alpha)}\}$, $\{b_l^{(\alpha)}\}$ and $\{c_l^{(\alpha)}\}$ defined in (65)-(67), respectively, it holds that

- $a_0^{(\alpha)} > a_1^{(\alpha)} > a_2^{(\alpha)} > \dots > a_l^{(\alpha)} > 0$ as $l \rightarrow \infty$, $a_0^{(\alpha)} \leq v_0$;
- $b_0^{(\alpha)} > b_1^{(\alpha)} > b_2^{(\alpha)} > \dots > b_l^{(\alpha)} > 0$ as $l \rightarrow \infty$;
- $c_2^{(\alpha)} > c_3^{(\alpha)} > c_4^{(\alpha)} > \dots > c_{k-1}^{(\alpha)} > 0$, $|c_l^{(\alpha)}| \leq v_0$ ($l = 0$ or 1), $c_2^{(\alpha)} \leq v_0$,

where $v_0 > 0$ is a constant.

Proof. From the definition of $a_l^{(\alpha)}$, we can verify that $a_0^{(\alpha)} = (\theta + 1)^{1-\alpha} - \theta^{1-\alpha}$ can be bounded by a constant $v_1 > 0$ and

$$a_l^{(\alpha)} = (1 - \alpha) \int_l^{l+1} (x + \theta)^{-\alpha} dx, \quad l = 0, 1, 2, \dots,$$

where $(x + \theta)^{-\alpha} > 0$ is a monotone decreasing function. Then it is no difficult to verify that

$$a_0^{(\alpha)} > a_1^{(\alpha)} > a_2^{(\alpha)} > \dots > a_l^{(\alpha)} > 0.$$

For the second conclusion and the first part of the third conclusion, the proofs are similar to that for Lemma 2.1 and Lemma 2.2 in [14]. Besides, in view of the definition (67) of $c_l^{(\alpha)}$, we have that

$$\begin{aligned} |c_0^{(\alpha)}| &= \left| \frac{(\theta+1)^{1-\alpha} - 3\theta^{1-\alpha}}{2} + \frac{(\theta+1)^{2-\alpha} - \theta^{2-\alpha}}{2-\alpha} \right| \\ &= \left| \frac{(\theta+1)^{1-\alpha} - 3\theta^{1-\alpha}}{2} + \frac{(2-\alpha)(\theta+\xi)^{1-\alpha}}{2-\alpha} \right| \leq \frac{3[(\theta+1)^{1-\alpha} + \theta^{1-\alpha}]}{2}, \end{aligned}$$

where $\xi \in (0, 1)$ and the mean value theorem has been used. It means $|c_0^{(\alpha)}|$ can be bounded by a constant $v_2 > 0$. Similarly, we can get there exists a constant $v_3 > 0$, such that

$$|c_1^{(\alpha)}| \leq \frac{3(\theta+2)^{1-\alpha} + 4(\theta+1)^{1-\alpha} + \theta^{1-\alpha}}{2} \leq v_3.$$

For $c_2^{(\alpha)}$, it follows

$$\begin{aligned} c_2^{(\alpha)} &= \frac{(\theta+3)^{1-\alpha} - 2(\theta+2)^{1-\alpha} + (\theta+1)^{1-\alpha}}{2} + \frac{(\theta+3)^{2-\alpha} - 2(\theta+2)^{2-\alpha} + (\theta+1)^{2-\alpha}}{2-\alpha} \\ &= \frac{(\theta+3)^{1-\alpha} - 2(\theta+2)^{1-\alpha} + (\theta+1)^{1-\alpha}}{2} + \frac{(2-\alpha)(\theta+\eta_2)^{1-\alpha} - (2-\alpha)(\theta+\eta_1)^{1-\alpha}}{2-\alpha} \\ &\leq \frac{3(\theta+3)^{1-\alpha} - 2(\theta+2)^{1-\alpha} - (\theta+1)^{1-\alpha}}{2} \leq v_4, \end{aligned}$$

where $\eta_1 \in (1, 2)$, $\eta_2 \in (2, 3)$ and $v_4 > 0$ is a constant. Hence, by setting $v_0 = \max_{1 \leq l \leq 4} v_l$ and summarizing the above results, all this completes the proof. \square

Next, we present the proof for Lemma 1.

Proof. Firstly, we consider the situation of $p = 0$. From (16), when $j = 0$, we have that

$$\begin{aligned} \gamma_{k,0}^{(0)} &= \frac{\mathcal{A}_{k,1} - \mathcal{A}_{k,0}}{h} = \frac{1}{h} \int_{t_k}^{t_{k+1}} (t_{k+1} - v)^{\alpha-1} [(v - t_1)^{1-\alpha} - (v - t_0)^{1-\alpha}] dv \\ &= \frac{(t_{k+\tilde{\theta}} - t_1)^{1-\alpha} - (t_{k+\tilde{\theta}} - t_0)^{1-\alpha}}{h} \int_{t_k}^{t_{k+1}} (t_{k+1} - v)^{\alpha-1} dv = -\frac{a_{k-1}^{(\alpha)}}{\alpha} < 0, \end{aligned}$$

where $t_{k+\tilde{\theta}} = (k + \tilde{\theta})h$, $\tilde{\theta} \in [0, 1]$ and the first mean value theorem for integrals has been used. For $j = 1, 2, \dots, k-1$, one has

$$\begin{aligned} \gamma_{k,j}^{(0)} &= \frac{\mathcal{A}_{k,j-1} - 2\mathcal{A}_{k,j} + \mathcal{A}_{k,j+1}}{h} \\ &= \frac{1}{h} \int_{t_k}^{t_{k+1}} (t_{k+1} - v)^{\alpha-1} [(v - t_{j-1})^{1-\alpha} - 2(v - t_j)^{1-\alpha} + (v - t_{j+1})^{1-\alpha}] dv \\ &= \frac{(t_{k+\tilde{\theta}} - t_{j-1})^{1-\alpha} - 2(t_{k+\tilde{\theta}} - t_j)^{1-\alpha} + (t_{k+\tilde{\theta}} - t_{j+1})^{1-\alpha}}{h} \int_{t_k}^{t_{k+1}} (t_{k+1} - v)^{\alpha-1} dv \\ &= \frac{a_{k-j}^{(\alpha)} - a_{k-j-1}^{(\alpha)}}{\alpha} < 0. \end{aligned}$$

For $j = k$, it holds that

$$\begin{aligned}\gamma_{k,k}^{(0)} &= \frac{\mathcal{A}_{k,k-1} - \mathcal{A}_{k,k}}{h} = \frac{1}{h} \int_{t_k}^{t_{k+1}} (t_{k+1} - v)^{\alpha-1} [(v - t_{k-1})^{1-\alpha} - (v - t_k)^{1-\alpha}] dv \\ &= \frac{(t_{k+\bar{\theta}} - t_{k-1})^{1-\alpha} - (t_{k+\bar{\theta}} - t_k)^{1-\alpha}}{h} \int_{t_k}^{t_{k+1}} (t_{k+1} - v)^{\alpha-1} dv = \frac{a_0^{(\alpha)}}{\alpha} > 0,\end{aligned}$$

and $\gamma_{k,k}^{(0)} = \frac{a_0^{(\alpha)}}{\alpha} \leq \frac{v_0}{\alpha}$, where Lemma 16 has been used. Similarly, for $\gamma_{k,j}^{(1)}$, by using the first mean value theorem for integrals, we obtain

$$\gamma_{k,j}^{(1)} = \begin{cases} -\frac{c_{k-1}^{(\alpha)}}{\alpha}, & j = 0, \\ \frac{-c_{k-j-1}^{(\alpha)} + c_{k-j}^{(\alpha)}}{\alpha}, & 1 \leq j \leq k-1, \\ \frac{c_0^{(\alpha)}}{\alpha}, & j = k. \end{cases}$$

This, together with Lemma 16, imply that $\gamma_{k,j}^{(1)} < 0$ ($0 \leq j \leq k-3$) and

$$\begin{aligned}|\gamma_{k,k-2}^{(1)}| &= \left| \frac{-c_1^{(\alpha)} + c_2^{(\alpha)}}{\alpha} \right| \leq \frac{2v_0}{\alpha}, \\ |\gamma_{k,k-1}^{(1)}| &= \left| \frac{-c_0^{(\alpha)} + c_1^{(\alpha)}}{\alpha} \right| \leq \frac{2v_0}{\alpha}, \quad |\gamma_{k,k}^{(1)}| = \left| \frac{c_0^{(\alpha)}}{\alpha} \right| \leq \frac{v_0}{\alpha}.\end{aligned}$$

Suppose that $u(t) = 1$ for $t \in [0, T]$, it follows from (16) that

$$\mathcal{H}^k(t_{k+1}) = \frac{1}{\Gamma(\alpha)\Gamma(2-\alpha)} \sum_{j=0}^k \gamma_{k,j}^{(0)} = \frac{1}{\Gamma(\alpha)\Gamma(2-\alpha)} \sum_{j=0}^k \gamma_{k,j}^{(1)} = 0,$$

so we get $\sum_{j=0}^k \gamma_{k,j}^{(0)} = 0$ and $\sum_{j=0}^k \gamma_{k,j}^{(1)} = 0$. Hence the lemma is proven. \square

B.2. Proof of Lemma 2.

Proof. It follows from (11) that

$$\begin{aligned}& \left| {}_{t_k} I_t^\alpha u(t) \Big|_{t=t_{k+1}} - h^\alpha \sum_{j=0}^p \beta_j^{(p)} u(t_{k+1-j}) \right| \\ &= \frac{1}{\Gamma(\alpha)} \left| \int_{t_k}^{t_{k+1}} (t_{k+1} - v)^{\alpha-1} \left[u(v) - \sum_{j=0}^p u(t_{k+1-j}) \prod_{i=0, i \neq j}^p \frac{v - t_{k+1-i}}{t_{k+1-j} - t_{k+1-i}} \right] dv \right| \\ &\leq \frac{1}{\Gamma(\alpha)} \left| \int_{t_k}^{t_{k+1}} (t_{k+1} - v)^{\alpha-1} u^{(p+1)}(\varsigma) \prod_{i=0}^p (v - t_{k+1-i}) dv \right| \\ &\leq \frac{h^{p+1} |u^{(p+1)}(\varsigma)|}{\Gamma(\alpha)} \left| \int_{t_k}^{t_{k+1}} (t_{k+1} - v)^{\alpha-1} dv \right| \leq v_5 h^{\alpha+p+1} t_{k+1}^{\sigma-p-1},\end{aligned}$$

where $\varsigma \in (t_k, t_{k+1})$ and $v_5 > 0$ is a constant independent of h . This completes the proof. \square

B.3. Proof of Lemma 3.

Proof. By (12), we have for $k = 2, 3, \dots, N-1$, $N \geq 3$ (the cases for $k = 0, 1$ are easy to check, so we omit these case here) that

$$\begin{aligned}
& \left| \mathcal{H}^k(t_{k+1}) - \mathcal{H}_0^k(t_{k+1}) \right| \\
&= \frac{1}{\Gamma(\alpha)\Gamma(1-\alpha)} \left| \int_{t_k}^{t_{k+1}} \frac{1}{(t_{k+1}-v)^{1-\alpha}} \sum_{j=0}^{k-1} \int_{t_j}^{t_{j+1}} \frac{u'(s) - (\Pi_{1,j}u(s))'}{(v-s)^\alpha} ds dv \right| \\
&\leq \frac{1}{\Gamma(\alpha)\Gamma(1-\alpha)} \left| \int_{t_k}^{t_{k+1}} \frac{1}{(t_{k+1}-v)^{1-\alpha}} \int_0^{t_1} \frac{u'(s) - (\Pi_{1,o}u(s))'}{(v-s)^\alpha} ds dv \right| \\
&\quad + \frac{1}{\Gamma(\alpha)\Gamma(1-\alpha)} \left| \int_{t_k}^{t_{k+1}} \frac{1}{(t_{k+1}-v)^{1-\alpha}} \sum_{j=1}^{\hat{k}-1} \int_{t_j}^{t_{j+1}} \frac{u'(s) - (\Pi_{1,j}u(s))'}{(v-s)^\alpha} ds dv \right| \\
&\quad + \frac{1}{\Gamma(\alpha)\Gamma(1-\alpha)} \left| \int_{t_k}^{t_{k+1}} \frac{1}{(t_{k+1}-v)^{1-\alpha}} \sum_{j=\hat{k}}^{k-1} \int_{t_j}^{t_{j+1}} \frac{u'(s) - (\Pi_{1,j}u(s))'}{(v-s)^\alpha} ds dv \right| \\
&:= \frac{1}{\Gamma(\alpha)\Gamma(1-\alpha)} (I_1 + I_2 + I_3),
\end{aligned}$$

where $\hat{k} \in (1, k)$. For I_1 , by using the integration by parts, one gets that

$$\begin{aligned}
I_1 &= \left| \int_{t_k}^{t_{k+1}} (t_{k+1}-v)^{\alpha-1} \int_0^{t_1} (v-s)^{-\alpha} d[u(s) - \Pi_{1,o}u(s)] dv \right| \\
&= \alpha \left| \int_{t_k}^{t_{k+1}} (t_{k+1}-v)^{\alpha-1} \int_0^{t_1} (v-s)^{-\alpha-1} \left[u(s) - \frac{s-t_1}{-t_1} u(0) - \frac{s}{t_1} u(t_1) \right] ds dv \right| \\
&= \alpha \left| \int_{t_k}^{t_{k+1}} (t_{k+1}-v)^{\alpha-1} \int_0^{t_1} (v-s)^{-\alpha-1} \left[\frac{s-t_1}{-t_1} \int_0^s u'(\tau) d\tau - \frac{s}{t_1} \int_s^{t_1} u'(\tau) d\tau \right] ds dv \right| \\
&= \alpha \sigma \left| \int_{t_k}^{t_{k+1}} (t_{k+1}-v)^{\alpha-1} \int_0^{t_1} (v-s)^{-\alpha-1} \left[\frac{s-t_1}{-t_1} \int_0^s \tau^{\sigma-1} d\tau - \frac{s}{t_1} \int_s^{t_1} \tau^{\sigma-1} d\tau \right] ds dv \right| \\
&\leq \alpha \left| \int_{t_k}^{t_{k+1}} (t_{k+1}-v)^{\alpha-1} \int_0^{t_1} (v-s)^{-\alpha-1} s^\sigma ds dv \right| \\
&\quad + \alpha \left| \int_{t_k}^{t_{k+1}} (t_{k+1}-v)^{\alpha-1} \int_0^{t_1} (v-s)^{-\alpha-1} (t_1^\sigma - s^\sigma) ds dv \right| \\
&\leq 3\alpha t_1^{\sigma+1} (t_k - t_1)^{-\alpha-1} \left| \int_{t_k}^{t_{k+1}} (t_{k+1}-v)^{\alpha-1} dv \right| = 3h^{\sigma+\alpha+1} t_{k-1}^{-\alpha-1}.
\end{aligned}$$

On the other hand, for I_2 , by using the mean value theorem and the Euler-Maclaurin formula, we arrive at

$$\begin{aligned}
I_2 &= \left| \int_{t_k}^{t_{k+1}} (t_{k+1}-v)^{\alpha-1} \sum_{j=1}^{\hat{k}-1} \int_{t_j}^{t_{j+1}} \frac{2s-t_j-t_{j+1}}{2(v-s)^\alpha} u''(\xi_j) ds dv \right| \\
&\leq \sigma(\sigma-1)h \left| \int_{t_k}^{t_{k+1}} (t_{k+1}-v)^{\alpha-1} \sum_{j=1}^{\hat{k}-1} t_j^{\sigma-2} \int_{t_j}^{t_{j+1}} (v-s)^{-\alpha} ds dv \right|
\end{aligned}$$

$$\begin{aligned}
&= \frac{\sigma(\sigma-1)h}{1-\alpha} \left| \int_{t_k}^{t_{k+1}} (t_{k+1}-v)^{\alpha-1} \sum_{j=1}^{\hat{k}-1} t_j^{\sigma-2} [(v-t_j)^{1-\alpha} - (v-t_{j+1})^{1-\alpha}] dv \right| \\
&\leq \sigma(\sigma-1)h \left| \int_{t_k}^{t_{k+1}} (t_{k+1}-v)^{\alpha-1} \sum_{j=1}^{\hat{k}-1} t_j^{\sigma-2} (v-t_{j+1})^{-\alpha} dv \right| \\
&\leq \sigma(\sigma-1)h \sum_{j=1}^{\hat{k}-1} t_j^{\sigma-2} (t_k-t_{j+1})^{-\alpha} \left| \int_{t_k}^{t_{k+1}} (t_{k+1}-v)^{\alpha-1} dv \right| \\
&\leq \frac{\sigma(\sigma-1)}{\alpha} h^{\alpha+1} t_k^{\sigma-\alpha-1},
\end{aligned}$$

where $\xi_j \in (t_j, t_{j+1})$ ($j = 1, 2, \dots, \hat{k}-1$). Next, it holds that

$$\begin{aligned}
I_3 &= \left| \int_{t_k}^{t_{k+1}} (t_{k+1}-v)^{\alpha-1} \sum_{j=\hat{k}}^{k-1} \int_{t_j}^{t_{j+1}} \frac{2s-t_j-t_{j+1}}{2(v-s)^\alpha} u''(\xi_j) ds dv \right| \\
&\leq \sigma(\sigma-1)h \left| \int_{t_k}^{t_{k+1}} (t_{k+1}-v)^{\alpha-1} \sum_{j=\hat{k}}^{k-1} t_j^{\sigma-2} \int_{t_j}^{t_{j+1}} (v-s)^{-\alpha} ds dv \right| \\
&= \frac{\sigma(\sigma-1)t_{\hat{k}}^{\sigma-2}h}{1-\alpha} \left| \int_{t_k}^{t_{k+1}} (t_{k+1}-v)^{\alpha-1} [(v-t_{\hat{k}})^{1-\alpha} - (v-t_k)^{1-\alpha}] dv \right| \\
&= \frac{\sigma(\sigma-1)t_{\hat{k}}^{\sigma-2}h}{1-\alpha} [(t_{k+\hat{\theta}}-t_{\hat{k}})^{1-\alpha} - (t_{k+\hat{\theta}}-t_k)^{1-\alpha}] \left| \int_{t_k}^{t_{k+1}} (t_{k+1}-v)^{\alpha-1} dv \right| \\
&\leq \frac{\sigma(\sigma-1)t_{\hat{k}}^{\sigma-2}h^{1+\alpha}}{\alpha(1-\alpha)} [(t_{k+\hat{\theta}}-t_{\hat{k}})^{1-\alpha} - (t_{k+\hat{\theta}}-t_k)^{1-\alpha}] \\
&\leq \frac{\sigma(\sigma-1)T}{\alpha(1-\alpha)} \left[\frac{1}{(k-\hat{k}+\hat{\theta})^\alpha} - \frac{1}{\hat{\theta}^\alpha} \right] h t_{\hat{k}}^{\sigma-2},
\end{aligned}$$

where $\hat{\theta} \in [0, 1]$, $\xi_j \in (t_j, t_{j+1})$ ($j = \hat{k}, \hat{k}+1, \dots, k-1$). Then for a suitable \hat{k} , there exists a constant $v_6 > 0$ independent of h such that

$$\begin{aligned}
|\mathcal{H}^k(t_{k+1}) - \mathcal{H}_0^k(t_{k+1})| &\leq \frac{1}{\Gamma(\alpha)\Gamma(1-\alpha)} \left\{ 3h^{\sigma+\alpha+1}t_{k-1}^{-\alpha-1} + \frac{\sigma(\sigma-1)}{\alpha} h^{\alpha+1}t_k^{\sigma-\alpha-1} \right. \\
&\quad \left. + \frac{\sigma(\sigma-1)T}{\alpha(1-\alpha)} \left[\frac{1}{(k-\hat{k}+\hat{\theta})^\alpha} - \frac{1}{\hat{\theta}^\alpha} \right] h t_{\hat{k}}^{\sigma-2} \right\} \\
&\leq v_6 (h^{\sigma+\alpha+1}t_{k+1}^{-\alpha-1} + h^{\alpha+1}t_{k+1}^{\sigma-\alpha-1} + h).
\end{aligned}$$

Similarly, we can get there exists a constant $v_7 > 0$ independent of h such that

$$|\mathcal{H}^k(t_{k+1}) - \mathcal{H}_1^k(t_{k+1})| \leq v_7 (h^{\sigma+\alpha+1}t_{k+1}^{-\alpha-1} + h^{\alpha+2}t_{k+1}^{\sigma-\alpha-2} + h^2).$$

Therefore, when setting $C_3 = \max\{v_7, v_8\}$, the lemma is proved. \square

B.4. Proof of Lemma 5.

Proof. From Lemma 2 we know that

$$\frac{h^\alpha t_k^{\sigma_r}}{\Gamma(\alpha+1)} {}_2F_1\left(-\sigma_r, 1; \alpha+1; -\frac{1}{k}\right) - h^\alpha \sum_{j=0}^p \beta_j^{(p)} t_{k+1-j}^{\sigma_r} = \mathcal{O}(h^{\alpha+p+1} t_{k+1}^{\sigma_r-p-1}),$$

which is equivalent to

$$\frac{k^{\sigma_r}}{\Gamma(\alpha+1)} {}_2F_1\left(-\sigma_r, 1; \alpha+1; -\frac{1}{k}\right) - \sum_{j=0}^p \beta_j^{(p)} (k+1-j)^{\sigma_r} = \mathcal{O}((k+1)^{\sigma_r-p-1}).$$

Hence, by (21), we have

$$\sum_{j=1}^{m_u} W_{k,j}^{(\alpha,\sigma,p)} j^{\sigma_r} = \mathcal{O}((k+1)^{\sigma_r-p-1}), \quad r = 1, 2, \dots, m_u.$$

Similarly, by using Lemma 2 and 3, we can obtain

$$\sum_{j=1}^{m_f} W_{k,j}^{(\alpha,\delta,p)} j^{\delta_r} = \mathcal{O}((k+1)^{\delta_r-p-1}), \quad r = 1, 2, \dots, m_f,$$

$$\sum_{j=1}^{\tilde{m}_u} \tilde{W}_{k,j}^{(\alpha,\sigma,p)} j^{\sigma_r} = \mathcal{O}((k+1)^{-\alpha-1}) + \mathcal{O}((k+1)^{\sigma_r-p-1}), \quad r = 1, 2, \dots, \tilde{m}_u.$$

Moreover, for $W_{k,j}^{(\delta,p)}$ in (41), we can get that

$$\sum_{j=1}^{\tilde{m}_f} W_{k,j}^{(\delta,0)} j^{\delta_r} = (k+1)^{\delta_r} - k^{\delta_r} = \mathcal{O}((k+1)^{\delta_r-1}), \quad r = 1, 2, \dots, \tilde{m}_f,$$

$$\sum_{j=1}^{\tilde{m}_f} W_{k,j}^{(\delta,1)} j^{\delta_r} = (k+1)^{\delta_r} - 2k^{\delta_r} + (k-1)^{\delta_r} = \mathcal{O}((k+1)^{\delta_r-2}), \quad r = 1, 2, \dots, \tilde{m}_f,$$

which ends the proof. \square

B.5. Proof of Theorem 6.

Proof. Let $e_{k+1} = u(t_{k+1}) - u_{k+1}$. When $p = 0$, subtracting (45) from (46) and using the Lipschitz condition (31) yield

$$\begin{aligned} \|e_{k+1}\|_\infty &\leq \|e_k\|_\infty + |\lambda| h^\alpha \left(\beta_0^{(0)} \|e_{k+1}\|_\infty + \sum_{j=1}^{m_u} \left| W_{k,j}^{(\alpha,\sigma,0)} \right| \|e_j\|_\infty \right) \\ &\quad - \frac{1}{\Gamma(\alpha)\Gamma(2-\alpha)} \sum_{j=0}^k \left| \gamma_{k,j}^{(0)} \right| \|e_j\|_\infty - \sum_{j=1}^{\tilde{m}_u} \left| \tilde{W}_{k,j}^{(\alpha,\sigma,0)} \right| \|e_j\|_\infty \\ &\quad + L\beta_0^{(0)} h^\alpha \left(\|e_k\|_\infty + \sum_{j=1}^{\tilde{m}_f} \left| W_{k,j}^{(\delta,0)} \right| \|e_j\|_\infty \right) \\ &\quad + Lh^\alpha \sum_{j=1}^{m_f} \left| W_{k,j}^{(\alpha,\delta,0)} \right| \|e_j\|_\infty + R_{k+1} \\ &\leq |\lambda| \beta_0^{(0)} h^\alpha \|e_{k+1}\|_\infty + \|e_k\|_\infty + L\beta_0^{(0)} h^\alpha \|e_k\|_\infty + \sum_{j=1}^M \tilde{W}_{k,j} \|e_j\|_\infty \\ &\quad - \frac{1}{\Gamma(\alpha)\Gamma(2-\alpha)} \sum_{j=0}^k \left| \gamma_{k,j}^{(0)} \right| \|e_j\|_\infty + R_{k+1}, \end{aligned} \tag{68}$$

where

$$\tilde{W}_{k,j} = |\lambda| h^\alpha \left| W_{k,j}^{(\alpha,\sigma,0)} \right| + L h^\alpha \left| W_{k,j}^{(\alpha,\delta,0)} \right| + \left| \tilde{W}_{k,j}^{(\alpha,\sigma,0)} \right| + L \beta_0^{(0)} h^\alpha \left| W_{k,j}^{(\delta,0)} \right|,$$

and

$$R_{k+1} = R_{k+1}^u + R_{k+1}^f + \tilde{R}_{k+1}^u + h^\alpha \beta_0^{(p)} \tilde{R}_{k+1}^f \leq v_9 h_0^q,$$

with $q_0 = \min \{1, \sigma_{\tilde{m}_u+1}, \sigma_{m_u+1} + \alpha, \delta_{m_f+1} + \alpha, \delta_{\tilde{m}_f+1} + \alpha\}$ and $v_9 > 0$ is a constant independent of h . It follows from Lemma 5 there exists a constant $v_{10} > 0$ such that

$$\tilde{W}_{k,j} \leq v_{10}, \quad \text{when } \sigma_{\tilde{m}_u} \leq 1, \sigma_{m_u}, \delta_{m_f}, \delta_{\tilde{m}_f} \leq \alpha + 1.$$

We rewrite (68) as

$$\begin{aligned} (1 - |\lambda| \beta_0^{(0)} h^\alpha) \|e_{k+1}\|_\infty &\leq (1 + L \beta_0^{(0)} h^\alpha) \|e_k\|_\infty + \sum_{j=1}^M \tilde{W}_{k,j} \|e_j\|_\infty \\ &\quad - \frac{1}{\Gamma(\alpha)\Gamma(2-\alpha)} \sum_{j=0}^k \left| \gamma_{k,j}^{(0)} \right| \|e_j\|_\infty + R_{k+1}. \end{aligned}$$

Since by using Lemma 1 we have

$$\sum_{j=0}^k \left| \gamma_{k,j}^{(0)} \right| = 2\gamma_{k,k}^{(0)} \leq 2C_1.$$

Then, when $|\lambda| \beta_0^{(p)} h^\alpha < 1$, we can obtain that

$$\begin{aligned} \|e_{k+1}\|_\infty &\leq \frac{1}{1 - |\lambda| \beta_0^{(0)} h^\alpha} \exp \left[1 + L \beta_0^{(0)} h^\alpha - \frac{2C_1}{\Gamma(\alpha)\Gamma(2-\alpha)} \right] \left(\sum_{j=1}^M \tilde{W}_{k,j} \|e_j\|_\infty + R_{k+1} \right) \\ &\leq v_{11} \left(\sum_{j=1}^M \tilde{W}_{k,j} \|e_j\|_\infty + R_{k+1} \right) \leq v_{11} \left(v_9 \sum_{j=1}^M \|e_j\|_\infty + v_{10} h^{q_0} \right), \end{aligned}$$

where the discrete Gronwall inequality in [18] has been used. For $p = 1$, we can also obtain that

$$\|e_{k+1}\|_\infty \leq v_{12} \left(\sum_{j=1}^M \|e_j\|_\infty + h^{q_1} \right),$$

with $q_1 = \min \{2, \sigma_{\tilde{m}_u+1} + 1, \sigma_{m_u+1} + \alpha + 1, \delta_{m_f+1} + \alpha + 1, \delta_{\tilde{m}_f+1} + \alpha + 1\}$ and v_{12} is a positive constant independent of h . Therefore, this completes the proof. \square

REFERENCES

- [1] M. ABRAMOWITZ AND I. A. STEGUN, *Handbook of Mathematical Functions: with Formulas, Graphs, and Mathematical Tables*, Courier Corporation, 1965.
- [2] R. P. AGARWAL, M. MEEHAN, AND D. O'REGAN, *Fixed Point Theory and Applications*, Cambridge University Press, 2001.
- [3] D. BAFFET AND J. S. HESTHAVEN, *High-order accurate adaptive kernel compression time-stepping schemes for fractional differential equations*, J. Sci. Comput., 72 (2017), pp. 1169–1195.

- [4] H. BRUNNER, *The numerical solution of weakly singular Volterra integral equations by collocation on graded meshes*, Math. Comp., 45 (1985), pp. 417–437.
- [5] H. BRUNNER, *On the numerical solution of nonlinear Volterra-Fredholm integral equations by collocation methods*, SIAM J. Numer. Anal., 27 (1990), pp. 987–1000.
- [6] W. CAO, F. ZENG, Z. ZHANG, AND G. E. KARNIADAKIS, *Implicit-explicit difference schemes for nonlinear fractional differential equations with nonsmooth solutions*, SIAM J. Sci. Comput., 38 (2016), pp. A3070–A3093.
- [7] W. DENG, *Short memory principle and a predictor-corrector approach for fractional differential equations*, J. Comput. Appl. Math., 206 (2007), pp. 174–188.
- [8] K. DIETHELM, *An algorithm for the numerical solution of differential equations of fractional order*, Electron. Trans. Numer. Anal., 5 (1997), pp. 1–6.
- [9] K. DIETHELM AND N. J. FORD, *Analysis of fractional differential equations*, J. Math. Anal. Appl., 265 (2002), pp. 229–248.
- [10] K. DIETHELM, N. J. FORD, AND A. D. FREED, *Detailed error analysis for a fractional Adams method*, Numer. Algorithms, 36 (2004), pp. 31–52.
- [11] T. FABER, A. JAISHANKAR, AND G. MCKINLEY, *Describing the firmness, springiness and rubberiness of food gels using fractional calculus. Part I: Theoretical framework*, Food Hydrocolloids, 62 (2017), pp. 311–324.
- [12] L. GALEONE AND R. GARRAPPA, *On multistep methods for differential equations of fractional order*, Mediterr. J. Math., 3 (2006), pp. 565–580.
- [13] L. GALEONE AND R. GARRAPPA, *Explicit methods for fractional differential equations and their stability properties*, J. Comput. Appl. Math., 228 (2009), pp. 548–560.
- [14] G. GAO, Z. SUN, AND H. ZHANG, *A new fractional numerical differentiation formula to approximate the Caputo fractional derivative and its applications*, J. Comput. Phys., 259 (2014), pp. 33–50.
- [15] R. GARRAPPA, *On linear stability of predictor-corrector algorithms for fractional differential equations*, Int. J. Comput. Math., 87 (2010), pp. 2281–2290.
- [16] R. GARRAPPA, *Trapezoidal methods for fractional differential equations: Theoretical and computational aspects*, Math. Comput. Simulation, 110 (2015), pp. 96–112.
- [17] W. GAUTSCHI, *Gauss quadrature approximations to hypergeometric and confluent hypergeometric functions*, J. Comput. Appl. Math., 139 (2002), pp. 173–187.
- [18] J. G. HEYWOOD AND R. RANNACHER, *Finite-element approximation of the nonstationary Navier-Stokes problem. Part IV: Error analysis for second-order time discretization*, SIAM J. Numer. Anal., 27 (1990), pp. 353–384.
- [19] A. JAISHANKAR AND G. H. MCKINLEY, *Power-law rheology in the bulk and at the interface: quasi-properties and fractional constitutive equations*, Proc. R. Soc. Lond. Ser. A Math. Phys. Eng. Sci., 469 (2013), p. 20120284.
- [20] E. KHARAZMI AND M. ZAYERNOURI, *Fractional pseudo-spectral methods for distributed-order fractional PDEs*, Int. J. Comput. Math., 95 (2018), pp. 1340–1361.
- [21] E. KHARAZMI AND M. ZAYERNOURI, *Fractional sensitivity equation method: Application to fractional model construction*, J. Sci. Comput., 80 (2019), pp. 110–140.
- [22] E. KHARAZMI, M. ZAYERNOURI, AND G. E. KARNIADAKIS, *Petrov-Galerkin and spectral collocation methods for distributed order differential equations*, SIAM J. Sci. Comput., 39 (2017), pp. A1003–A1037.
- [23] E. KHARAZMI, M. ZAYERNOURI, AND G. E. KARNIADAKIS, *A Petrov-Galerkin spectral element method for fractional elliptic problems*, Comput. Methods Appl. Mech. Eng., 324 (2017), pp. 512–536.
- [24] Y. LIN AND C. XU, *Finite difference/spectral approximations for the time-fractional diffusion equation*, J. Comput. Phys., 225 (2007), pp. 1533–1552.
- [25] A. LISCHKE, M. ZAYERNOURI, AND G. E. KARNIADAKIS, *A Petrov-Galerkin spectral method of linear complexity for fractional multiterm ODEs on the half line*, SIAM J. Sci. Comput., 39 (2017), pp. A922–A946.
- [26] X. LU, H. PANG, AND H. SUN, *Fast approximate inversion of a block triangular Toeplitz matrix with applications to fractional sub-diffusion equations*, Numer. Linear Algebra Appl., 22 (2015), pp. 866–882.
- [27] C. LUBICH, *On the stability of linear multistep methods for Volterra convolution equations*, IMA J. Numer. Anal., 3 (1983), pp. 439–465.
- [28] C. LUBICH, *Discretized fractional calculus*, SIAM J. Math. Anal., 17 (1986), pp. 704–719.
- [29] C. LUBICH, *A stability analysis of convolution quadrature for Abel-Volterra integral equations*, IMA J. Numer. Anal., 6 (1986), pp. 87–101.
- [30] C. LUBICH AND A. SCHÄDLE, *Fast convolution for nonreflecting boundary conditions*, SIAM J. Sci. Comput., 24 (2002), pp. 161–182.

- [31] F. MAINARDI, *Fractional Calculus and Waves in Linear Viscoelasticity: An Introduction to Mathematical Models*, World Scientific, 2010.
- [32] F. MERAL, T. ROYSTON, AND R. MAGIN, *Fractional calculus in viscoelasticity: an experimental study*, Commun. Nonlinear Sci. Numer. Simul., 15 (2010), pp. 939–945.
- [33] M. NAGHIBOLHOSSEINI, *Estimation of outer-middle ear transmission using DPOAEs and fractional-order modeling of human middle ear*, PhD thesis, City University of New York, NY., 2015.
- [34] M. NAGHIBOLHOSSEINI AND G. R. LONG, *Fractional-order modelling and simulation of human ear*, Int. J. Comput. Math., 95 (2018), pp. 1257–1273.
- [35] J. W. PEARSON, *Computation of hypergeometric functions*, PhD thesis, University of Oxford, 2009.
- [36] I. PODLUBNY, *Fractional Differential Equations*, San Diego, CA, USA: Academic Press, 1999.
- [37] C. F. RODRIGUES, J. L. SUZUKI, AND M. L. BITTENCOURT, *Construction of minimum energy high-order Helmholtz bases for structured elements*, J. Comput. Phys., 306 (2016), pp. 269–290.
- [38] M. SAMIEE, E. KHARAZMI, M. ZAYERNOURI, AND M. M. MEERSCHAERT, *Petrov-Galerkin method for fully distributed-order fractional partial differential equations*, arXiv preprint arXiv:1805.08242, (2018).
- [39] M. SAMIEE, M. ZAYERNOURI, AND M. M. MEERSCHAERT, *A unified spectral method for FPDEs with two-sided derivatives; part I: a fast solver*, J. Comput. Phys., 385 (2019), pp. 225–243.
- [40] M. SAMIEE, M. ZAYERNOURI, AND M. M. MEERSCHAERT, *A unified spectral method for FPDEs with two-sided derivatives; Part II: Stability, and error analysis*, J. Comput. Phys., 385 (2019), pp. 244–261.
- [41] A. SCHÄDLE, M. LÓPEZ-FERNÁNDEZ, AND C. LUBICH, *Fast and oblivious convolution quadrature*, SIAM J. Sci. Comput., 28 (2006), pp. 421–438.
- [42] F. SONG, C. XU, AND G. E. KARNIADAKIS, *A fractional phase-field model for two-phase flows with tunable sharpness: Algorithms and simulations*, Comput. Methods Appl. Mech. Eng., 305 (2016), pp. 376–404.
- [43] M. STYNES, E. O’RIORDAN, AND J. L. GRACIA, *Error analysis of a finite difference method on graded meshes for a time-fractional diffusion equation*, SIAM J. Numer. Anal., 55 (2017), pp. 1057–1079.
- [44] J. SUZUKI, *Aspects of fractional-order modeling and efficient bases to simulate complex materials using finite element methods*, PhD thesis, University of Campinas, Brazil., 2017, <http://repositorio.unicamp.br/jspui/handle/REPOSIP/330675>.
- [45] J. SUZUKI AND M. BITTENCOURT, *Application of the hp-FEM for Hyperelastic Problems with Isotropic Damage*, Springer International Publishing, 2016, pp. 113–150.
- [46] J. SUZUKI AND P. MUÑOZ ROJAS, *Transient analysis of geometrically non-linear trusses considering coupled plasticity and damage*, Tenth World Congress on Computational Mechanics, 1 (2014), pp. 322–341.
- [47] J. SUZUKI AND M. ZAYERNOURI, *An automated singularity-capturing scheme for fractional differential equations*, arXiv preprint arXiv:1810.12219, (2018).
- [48] J. SUZUKI, M. ZAYERNOURI, M. BITTENCOURT, AND G. KARNIADAKIS, *Fractional-order uniaxial visco-elasto-plastic models for structural analysis*, Comput. Methods Appl. Mech. Eng., 308 (2016), pp. 443–467.
- [49] T. TANG, *A finite difference scheme for partial integro-differential equations with a weakly singular kernel*, Appl. Numer. Math., 11 (1993), pp. 309–319.
- [50] P. VARGHAEI, E. KHARAZMI, J. SUZUKI, AND M. ZAYERNOURI, *Vibration analysis of geometrically nonlinear and fractional viscoelastic cantilever beams*, arXiv preprint arXiv:1909.02142, (2019).
- [51] Z. XU AND W. CHEN, *A fractional-order model on new experiments of linear viscoelastic creep of Hami Melon*, Comput. Math. Appl., 66 (2013), pp. 677–681.
- [52] Y. YU, P. PERDIKARIS, AND G. E. KARNIADAKIS, *Fractional modeling of viscoelasticity in 3D cerebral arteries and aneurysms*, J. Comput. Phys., 323 (2016), pp. 219–242.
- [53] S. B. YUSTE AND J. QUINTANA-MURILLO, *A finite difference method with non-uniform timesteps for fractional diffusion equations*, Comput. Phys. Commun., 183 (2012), pp. 2594–2600.
- [54] M. ZAYERNOURI, W. CAO, Z. ZHANG, AND G. E. KARNIADAKIS, *Spectral and discontinuous spectral element methods for fractional delay equations*, SIAM J. Sci. Comput., 36 (2014), pp. B904–B929.
- [55] M. ZAYERNOURI AND G. E. KARNIADAKIS, *Exponentially accurate spectral and spectral element methods for fractional ODEs*, J. Comput. Phys., 257 (2014), pp. 460–480.
- [56] M. ZAYERNOURI AND G. E. KARNIADAKIS, *Fractional spectral collocation methods for linear and nonlinear variable order FPDEs*, J. Comput. Phys., 293 (2015), pp. 312–338.

- [57] M. ZAYERNOURI AND A. MATZAVINOS, *Fractional Adams-Bashforth/Moulton methods: An application to the fractional Keller-Segel chemotaxis system*, J. Comput. Phys., 317 (2016), pp. 1–14.
- [58] F. ZENG, C. LI, F. LIU, AND I. TURNER, *Numerical algorithms for time-fractional subdiffusion equation with second-order accuracy*, SIAM J. Sci. Comput., 37 (2015), pp. A55–A78.
- [59] F. ZENG, I. TURNER, AND K. BURRAGE, *A stable fast time-stepping method for fractional integral and derivative operators*, J. Sci. Comput., 77 (2018), pp. 283–307.
- [60] F. ZENG, I. TURNER, K. BURRAGE, AND G. E. KARNIADAKIS, *A new class of semi-implicit methods with linear complexity for nonlinear fractional differential equations*, SIAM J. Sci. Comput., 40 (2018), pp. A2986–A3011.
- [61] F. ZENG, Z. ZHANG, AND G. E. KARNIADAKIS, *Second-order numerical methods for multi-term fractional differential equations: smooth and non-smooth solutions*, Comput. Methods Appl. Mech. Eng., 327 (2017), pp. 478–502.
- [62] Y. ZHANG, H. SUN, H. H. STOWELL, M. ZAYERNOURI, AND S. E. HANSEN, *A review of applications of fractional calculus in Earth system dynamics*, Chaos Solitons Fractals, 102 (2017), pp. 29–46.
- [63] Y. ZHANG, Z. SUN, AND H. LIAO, *Finite difference methods for the time fractional diffusion equation on non-uniform meshes*, J. Comput. Phys., 265 (2014), pp. 195–210.
- [64] Y. ZHOU AND L. PENG, *On the time-fractional Navier-Stokes equations*, Comput. Math. Appl., 73 (2017), pp. 874–891.
- [65] Y. ZHOU AND C. ZHANG, *Convergence and stability of block boundary value methods applied to nonlinear fractional differential equations with Caputo derivatives*, Appl. Numer. Math., 135 (2019), pp. 367–380.
- [66] Y. ZHOU AND C. ZHANG, *One-leg methods for nonlinear stiff fractional differential equations with Caputo derivatives*, Appl. Math. Comput., 348 (2019), pp. 594–608.
- [67] Y. ZHOU, C. ZHANG, AND L. BRUGNANO, *Preconditioned quasi-compact boundary value methods for space-fractional diffusion equations*, Numer. Algorithms, (2019), <https://doi.org/10.1007/s11075-019-00773-z>.
- [68] Y. ZHOU, C. ZHANG, AND H. WANG, *Boundary value methods for Caputo fractional differential equations*, J. Comput. Math. (in press), (2019).